

## Existence, Functional Impairment, and Lung Repair Potential of Endothelial Colony-Forming Cells in Oxygen-Induced Arrested Alveolar Growth

Rajesh S. Alphonse, MD, PhD; Arul Vadivel, PhD; Moses Fung, BSc; William Chris Shelley, BSc; Paul John Critser, MD, PhD; Lavinia Ionescu, PhD; Megan O'Reilly, PhD; Robin K. Ohls, MD; Suzanne McConaghy, MSc; Farah Eaton, BSc; Shumei Zhong, MSc; Merv Yoder, MD; Bernard Thébaud, MD, PhD

**Background**—Bronchopulmonary dysplasia and emphysema are life-threatening diseases resulting from impaired alveolar development or alveolar destruction. Both conditions lack effective therapies. Angiogenic growth factors promote alveolar growth and contribute to alveolar maintenance. Endothelial colony-forming cells (ECFCs) represent a subset of circulating and resident endothelial cells capable of self-renewal and de novo vessel formation. We hypothesized that resident ECFCs exist in the developing lung, that they are impaired during arrested alveolar growth in experimental bronchopulmonary dysplasia, and that exogenous ECFCs restore disrupted alveolar growth.

**Methods and Results**—Human fetal and neonatal rat lungs contain ECFCs with robust proliferative potential, secondary colony formation on replating, and de novo blood vessel formation in vivo when transplanted into immunodeficient mice. In contrast, human fetal lung ECFCs exposed to hyperoxia in vitro and neonatal rat ECFCs isolated from hyperoxic alveolar growth-arrested rat lungs mimicking bronchopulmonary dysplasia proliferated less, showed decreased clonogenic capacity, and formed fewer capillary-like networks. Intrajugular administration of human cord blood-derived ECFCs after established arrested alveolar growth restored lung function, alveolar and lung vascular growth, and attenuated pulmonary hypertension. Lung ECFC colony- and capillary-like network-forming capabilities were also restored. Low ECFC engraftment and the protective effect of cell-free ECFC-derived conditioned media suggest a paracrine effect. Long-term (10 months) assessment of ECFC therapy showed no adverse effects with persistent improvement in lung structure, exercise capacity, and pulmonary hypertension.

**Conclusions**—Impaired ECFC function may contribute to arrested alveolar growth. Cord blood-derived ECFC therapy may offer new therapeutic options for lung diseases characterized by alveolar damage. (*Circulation*. 2014;129:2144-2157.)

**Key Words:** angiogenesis inducing agents ■ hypertension, pulmonary ■ lung diseases ■ stem cells

Despite improvements in the ability to control fertility, treat infertility, and reduce maternal, fetal, and infant mortality, neither the preterm birth rate nor the rate of long-term disabilities associated with extreme preterm birth has declined.<sup>1</sup> Preterm delivery remains a major healthcare problem, affecting 10% of all births and accounting for >85% of all perinatal complications and death. Each year, 5000 to 10000 newborns have bronchopulmonary dysplasia (BPD), a chronic lung disease that follows ventilator and oxygen therapy for acute respiratory failure after preterm birth. BPD is characterized by interrupted development of alveolar structures and can be complicated by pulmonary hypertension.<sup>2</sup> BPD has

long-term consequences that extend into adulthood, including early-onset emphysema, and currently lacks specific therapeutic options.<sup>3,4</sup> Understanding how alveoli and the underlying capillary network develop and how these mechanisms are disrupted in disease states is critical for developing effective therapies for lung regeneration.

**Editorial see p 2091  
Clinical Perspective on p 2157**

Emerging evidence indicates that endothelial-derived angiocrine signals induce and sustain regenerative lung alveolarization.<sup>5</sup> Vascular endothelial growth factor (VEGF) is

Received May 24, 2013; accepted February 21, 2014.

From the Department of Pediatrics, Women and Children's Health Research Institute, Cardiovascular Research Center and Pulmonary Research Group, University of Alberta, Edmonton, Canada (R.S.A., M.F., L.I. M.O., F.E.); Ottawa Hospital Research Institute, Regenerative Medicine Program, Sprott Center for Stem Cell Research, Department of Pediatrics, Children's Hospital of Eastern Ontario, University of Ottawa, Ottawa, Ontario, Canada (A.V., S.Z., B.T.); Department of Pediatrics, Herman B Wells Center for Pediatrics Research, Division of Neonatal-Perinatal Medicine, Indiana University School of Medicine, Indianapolis, IN (W.C.S., P.J.C., M.Y.); and Department of Pediatrics, University of New Mexico, Albuquerque, NM (R.K.O., S.M.).

The online-only Data Supplement is available with this article at <http://circ.ahajournals.org/lookup/suppl/doi:10.1161/CIRCULATIONAHA.114.009124/-/DC1>.

Correspondence to Bernard Thébaud, MD, PhD, Ottawa Hospital Research Institute, 501 Smyth Rd, Ottawa, ON K1H 8L6, Canada. E-mail [bthebaud@ohri](mailto:bthebaud@ohri)  
© 2014 American Heart Association, Inc.

*Circulation* is available at <http://circ.ahajournals.org>

DOI: 10.1161/CIRCULATIONAHA.114.009124

absolutely critical for vascular development and embryonic survival. VEGF signaling contributes to normal lung development, and early disruption of VEGF signaling leads to structural abnormalities seen in experimental and human BPD and emphysema. Angiogenic growth factor activation protects against O<sub>2</sub>-induced arrested alveolarization and stimulates lung vascular growth in newborn rats.<sup>6,7</sup> Compensatory lung growth following unilateral pneumonectomy stimulates pulmonary capillary endothelial cells to produce angiocrine growth factors that induce the proliferation of epithelial progenitor cells to support alveolarization.<sup>8</sup>

Recent observations suggest that the lung microvascular endothelium is enriched with resident progenitor cells that exhibit vasculogenic capacity.<sup>9</sup> These highly proliferative cells resemble the endothelial colony-forming cells (ECFCs) described in human peripheral and umbilical cord blood.<sup>10</sup> The role of lung ECFCs during normal and impaired lung growth is unknown.

We hypothesized that ECFC-driven angiogenesis contributes to normal lung alveolar development, and ECFC supplementation restores disrupted lung alveolar and vascular growth in hyperoxia-induced experimental BPD.

## Materials and Methods

Expanded methods are available in the online-only Data Supplement. All procedures were approved by the Animal Health Care Committee of the University of Alberta. Human fetal tissue collection was reviewed by the Institutional Review Board at the University of New Mexico.

## Lung ECFC Isolation and Culture

Human fetal lungs (n=3, 17–20 weeks gestational age) were collected within 60 minutes after termination, washed in sterile phosphate-buffered saline with antimicrobials, and suspended for further processing in Minimal Essential Medium-a with 10% fetal calf serum and antimicrobials. Rat lungs were collected at postnatal day (P) 14 (n=5/group). Under aseptic conditions, the peripheral rims of the lungs were cut out, chopped into 1- to 2-mm<sup>2</sup> pieces, and suspended in digestive solution (0.1 U collagenase and 0.8 U dispase/mL; Roche Applied Science, Laval, QC) at 37°C for 1 hour with intermittent shaking. The lung digest was strained through 70-mm and 40-mm cell strainers in tandem and washed twice with Dulbecco's modified Eagle medium (DMEM) plus 10% fetal calf serum, at 300g and 4°C for 10 minutes. After washing, the cells were resuspended in phosphate-buffered saline containing 0.1% (wt/vol) bovine serum albumin and incubated with streptavidin-tagged Dynabeads (Dyna, Invitrogen, Burlington, ON) that were pretreated with biotinylated anti-rat or anti-human CD31 antibody (Abcam, Cambridge, MA). The Dynabead-tagged CD31-positive cells were selected by using a magnetic separator and plated in a 6-well plate (4000–5000 cells/well) precoated with rat tail collagen type I and placed in a 37°C, 5% CO<sub>2</sub> humidified incubator. After 24 hours of culture, nonadherent cells and debris were aspirated, and adherent cells were washed once and added with complete Endothelial Growth Medium-2. Medium was changed daily for 7 days and then every other day up to 14 days. ECFC colonies appeared as a well-circumscribed monolayer of cobblestone-appearing cells, between 5 and 14 days. ECFC colonies were identified daily from day 5 and enumerated on day 7 by visual inspection by using an inverted microscope (Olympus, Lake Success, NY), under ×20 magnification. Individual ECFC colonies were marked with a fine-tipped marker and clonally isolated by using cloning cylinders (Fisher Scientific, Ottawa, ON) and plated in T<sub>25</sub> flasks pretreated with collagen type I. On confluence, ECFCs were plated and expanded in type I collagen-coated T<sub>75</sub> flasks. ECFCs between passages 4 and 8 were used for all experiments.

## Dil-Acetylated Low-Density Lipoprotein Uptake and *Ulex europaeus*-Lectin Binding

Experiments were performed as previously described.<sup>10</sup>

## Immunophenotyping of ECFCs

ECFCs were phenotyped by flow cytometry analysis.<sup>10</sup>

## Retroviral Mediated Enhanced Green Fluorescent Protein Labeling of ECFCs

Rat lung ECFCs in passage 4 to 5 were incubated overnight with 2 × 10<sup>6</sup> TU/mL of lentiviral vector and 7 μg/mL protamine sulfate in complete Endothelial Growth Medium-2. ECFCs in wells with uniform green fluorescence were trypsinized, expanded, and sorted for green fluorescence protein by using fluorescent-activated cell sorting.

## In Vitro Cell Viability Assay

ECFC viability was evaluated at various time points with the use of the 3-(4,5-dimethylthiazol-2-yl)-2,5-diphenyl tetrazolium bromide assay as previously described.<sup>11</sup>

## Capillary-Like Network Formation in Matrigel

The formation of cordlike structures by ECFCs was assessed on Matrigel (BD Biosciences, Mississauga, ON) coated 96-well tissue culture plates as previously described.<sup>7</sup>

## Single-Cell Clonogenicity

The FACSaria cell sorter (BD Biosciences, Mississauga, ON) was used to place 1 ECFC per well in a flat-bottomed 96-well tissue culture plate precoated with type I collagen and containing 200 μL of complete Endothelial Growth Medium-2. At day 14, Hoechst 33258 (Sigma) was added at 3 μg/mL to each well for 10 minutes for nuclear detection. The culture plate was examined with a fluorescent microscope at ×20 magnification, well by well, for the growth of endothelial cells.

## De Novo Angiogenesis in Vivo

ECFCs were loaded on collagen-fibronectin matrices and implanted subcutaneously in nonobese diabetic/severe combined immunodeficiency mice to assess their capacity to contribute to de novo vasculogenesis as described.<sup>12</sup>

## Oxygen-Induced BPD Model

We used 3 rodent models of oxygen-induced BPD. (1) For comparison of lung ECFC function, newborn Sprague Dawley rat pups were exposed to room air (21%; control group) or hyperoxia (95% oxygen; BPD group) from birth to P14 in sealed Plexiglas chambers (OxyCycler; Biospherix, Lacona, NY) with continuous oxygen monitoring, and ECFCs were isolated at P14 for comparative analysis.<sup>7</sup> (2) To test the therapeutic potential of human cord blood-derived ECFCs, immune-compromised newborn rag<sup>-/-</sup> mice were exposed to 85% oxygen from P4 to P14. Human cord blood-derived ECFCs, isolated, expanded, and quality controlled as previously described,<sup>10</sup> were administered at P14 through the jugular vein (10<sup>5</sup> cells/mouse in 100 μL of DMEM). Lungs were harvested at P28. For cell engraftment experiments, ECFCs were labeled before an injection with a red fluorophore (CellBrite Cytoplasmic Membrane Staining Kit, Biotium Inc, Hayward, CA). A subset of rag<sup>-/-</sup> mice was kept for long-term assessment until 10 months of age. (3) In subsequent experiments, we used RNU nude rats (exposed to 95% oxygen from P4 to P14 and injected with 2.5 × 10<sup>5</sup> cells/rat in 100 μL of DMEM) to test if human cord blood-derived ECFC treatment restored resident lung ECFC function.

## Lung Morphometry

Lungs were fixed and alveolar structures were quantified on a motorized microscope stage (Leica CTRMIC and openlab software, Quorum Technologies; Guelph, ON) by using the mean linear intercept as previously described.<sup>7</sup>

## Immunohistochemistry

von Willebrand Factor–positive lung capillaries (30–100  $\mu\text{m}$ ) were quantified on a motorized microscope stage.

## Right Ventricular Hypertrophy

The right ventricle free wall was separated from the left ventricle and the septal wall. The tissue was dried overnight and weighed the following day.<sup>13</sup>

## Echocardiography

All evaluations of pulmonary artery flow were performed with a (maximal) sweep speed of 200 mm/s. Pulsed-wave Doppler of pulmonary outflow was recorded in the parasternal view at the pulmonary valve level. The pulmonary arterial acceleration time (PAAT) was measured from the beginning of the pulmonary flow to its onset and normalized with heart rate for comparisons as described.<sup>13</sup>

## Lung Function Testing

Tests were performed on anesthetized and paralyzed animals with the use of Flexivent (Scireq, Montreal, QC, Canada) as described.<sup>14</sup>

## Real-Time Polymerase Chain Reaction

Real-time polymerase chain reaction was performed on frozen lungs from 3 animals/group harvested at various time points after injection as described.<sup>15</sup>

## ECFC-Derived Conditioned Medium Experiments

Conditioned medium (CdM) was obtained as described.<sup>15</sup> On preparation, CdM was pooled, frozen at  $-80^{\circ}\text{C}$  and thawed right before use. Control cell CdM was obtained from human umbilical vein endothelial cells (HUVECs).

In vitro, AT2 were isolated from time-dated fetal day 19.5 rat lungs as described by using serial differential adhesions to plastic and low-speed centrifugations.<sup>16</sup> For wound-healing assays, a cell monolayer was scraped with a p200 pipette tip and media replaced with CdM or DMEM as described.<sup>16</sup>

In vivo, CdM was administered daily to newborn rats exposed to hyperoxia through intraperitoneal injections at the dose of  $7 \mu\text{L/g}^{15}$  from P4 to P21 and lungs were harvested at P22.

## Exercise Capacity

Mice were run according to a predetermined protocol.<sup>15</sup>

## Statistical Analysis

Values are expressed as means $\pm$ standard error of the mean. Statistical comparisons were made with 1-way analysis of variance. Time course studies were analyzed by using repeated-measures analysis of variance. Post hoc analysis used Fisher probable least significant difference test (Statview 5.1; Abacus Concepts, Berkeley, CA). A value of  $P < 0.05$  was considered statistically significant. All  $P$  values were 2-sided, and no adjustment for multiple comparisons was made. All end points were assessed by investigators blinded to the experimental groups.

## Results

### Human Fetal Lung Harbors ECFCs With Self-Renewal, High Proliferative Potential, and de Novo Blood Vessel Formation Capacity

CD31-positive selected cells isolated from human fetal lung tissue yielded cobblestone-like colonies at between 4 and

14 days in culture (Figure 1A). These late-outgrowth colonies demonstrated basic endothelial cell characteristics such as ingestion of Dil-acLDL, binding *U europaeus*-lectin (Figure 1B) and tube formation in Matrigel (Figure 1C). Further phenotypic characterization revealed the expression of endothelial-specific cell surface markers including CD31, CD105 (endoglin), CD144 (VE-cadherin), and CD146 (M-CAM; Figure 1D). Human ECFCs were negative for monocyte/macrophage-specific CD14 and hematopoietic cell-specific CD45 (Figure 1D) and, thus, display an ECFC-like phenotype, consistent with the phenotype of circulating human cord blood ECFC.<sup>17</sup>

In single-cell clonogenic assays, lung endothelial cells generated colonies from single-plated cells:  $6.0 \pm 1.0\%$  formed colonies with 50 to 500 cells (low proliferative potential) and  $7.6 \pm 2.8\%$  formed  $>500$  cells (high proliferative potential, HPP) in 3 independent experiments (Figure 1E). On replating, ECFCs generated secondary colonies with similar frequency ( $6.0 \pm 1.0\%$  colonies with 50–500 cells and  $8.0 \pm 2.0\%$  formed  $>500$  cells) in 3 independent experiments (Figure 1F). Thus, the human lung endothelial cells displayed the clonal self-replenishing capacity.

In collagen-fibronectin–loaded matrices implanted subcutaneously in nonobese diabetic/severe combined immunodeficiency mice, human lung ECFCs formed de novo capillaries identified by antibody specific for human CD31 that connected with the host vasculature as demonstrated by the presence of circulating red blood cells in the capillary lumen (Figure 1G). Together these observations confirm the existence of resident ECFCs with properties similar to cord blood ECFC in the developing human lung.

### Hyperoxia Impairs Human Lung ECFC Function

Hyperoxia is 1 deleterious factor contributing to BPD. To mimic the disease condition in vitro, we exposed human lung ECFCs to 40% hyperoxia for 24 hours. ECFCs exposed to hyperoxia formed fewer capillary-like structures in Matrigel in comparison with ECFCs exposed to room air (Figure 1H) and generated fewer HPP ECFC colonies in comparison with ECFCs cultured in room air (Figure 1I). These results are consistent with previous studies reporting disrupted VEGF-nitric oxide signaling in cord blood ECFC exposed to hyperoxia in vitro and suggests impaired ECFC function may be associated with decreased lung vascular growth and arrested alveolarization in BPD.

### Lung ECFC Function Is Impaired in Experimental Hyperoxia-Induced BPD in Newborn Rats

To further investigate this hypothesis, we explored lung ECFC function in a well-established hyperoxia-induced neonatal rat model of arrested alveolar growth mimicking some of the histological features seen in human BPD.

First, we show that, similar to the human fetal lung, the neonatal rat lung harbors ECFCs that form cobblestone-like colonies within 7 to 14 days, with basic endothelial cell characteristics (Dil-acLDL ingestion and *U europaeus*-lectin binding) and tubelike formation in Matrigel (Figure 2A through 2C). The lung ECFC also displayed endothelial-specific cell surface markers (CD31, VEGFR2, and von Willebrand Factor) but did not express hematopoietic cell-specific CD45, CD14, or CD133



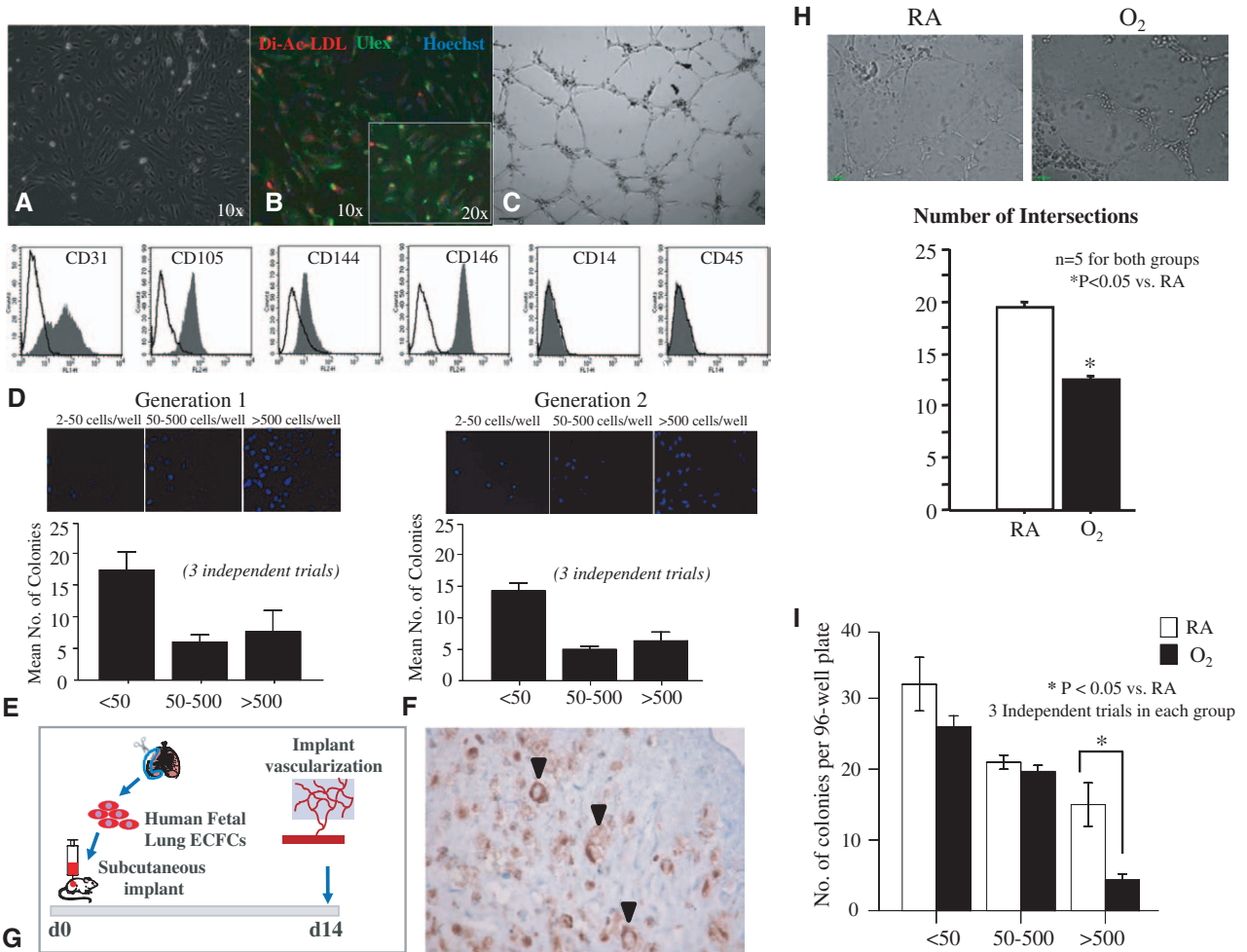


**Figure 1.** ECFCs exist in the developing human fetal lung and are perturbed by hyperoxia. **A**, Phase-contrast microscopy showing characteristic cobblestone-like colonies of CD31-positive cells obtained by beads isolation. **B**, These cells demonstrate Dil-acLDL uptake (red) within 4 hours of incubation and *Ulex europaeus*-lectin binding (green) within 1 hour of incubation after fixation. Counterstaining with Hoechst 33258 (blue) illustrates that all adherent cells are positive for LDL uptake and *U. europaeus* (Ulex)-lectin binding. **C**, These cells form tube-like structures when suspended in Matrigel. **D**, Fluorescent-activated cell sorting. Isolated cells are positive for endothelial-specific cell surface antigens CD31, CD105 (endoglin), CD144 (VE-cadherin), CD146 (M-CAM), and negative for monocyte/macrophage-specific CD14 and hematopoietic cell-specific CD45. Filled gray histograms represent antigen staining with negative isotype controls overlaid in white. All experiments were performed in triplicate. **E**, Single-cell clonogenic assay. Single cells are capable of giving rise to clusters (up to 50 cells) or colonies 50 to 500 cells (low proliferative potential, LPP) or more than 500 cells (high proliferative potential, HPP) in 96-well plates when plated at a seeding density of 1 cell per well. Results represent the mean  $\pm$  standard error of mean of 3 independent experiments. **F**, On replating, HPP ECFCs were able to form clusters or secondary colonies with LPP and HPP. **G**, Subcutaneous Matrigel Plug Assay. Human fetal lung ECFCs form blood vessels de novo when seeded in fibronectin-collagen plugs ( $10^6$  ECFCs per implant) and implanted subcutaneously into the flanks of NOD/SCID mice. Fourteen days postimplantation, the cellularized implants were excised, paraffin embedded, and stained with hematoxylin and eosin and anti-human CD31 (brown). Black arrows indicate red blood cell-perfused anti-human CD31+ vessels within the gel implant. **H**, Hyperoxia impairs network formation in vitro. Human fetal lung ECFCs exposed to 40% hyperoxia in vitro show a significant decrease in the number of intersects in comparison with RA-exposed ECFCs ( $n=5$  for each group,  $*P<0.05$ ). **I**, Comparative single-cell clonogenic assay. Human fetal lung ECFC exposed to 40% hyperoxia in vitro and plated in 96-well plates at a seeding density of 1 cell per well formed clusters and gave rise to colonies with LPP, but formed significantly fewer HPP than RA-exposed ECFCs ( $*P<0.05$ , 3 independent experiments). Dil-acLDL indicates Dil-acetylated low-density lipoprotein; ECFC, endothelial colony-forming cell; LDL, low-density lipoprotein; NOD/SCID, nonobese diabetic/severe combined immunodeficiency; and RA, room air.

(Figure 2D). In single-cell clonogenic assays, rat ECFCs generated low proliferative potential and HPP colonies from single-plated cells and secondary HPP on replating (Figure 2E).

Rat lung ECFCs also formed de novo capillaries when implanted subcutaneously in nonobese diabetic/severe combined immunodeficiency mice in collagen-fibronectin-loaded matrices (Figure 2F).

Next, we compared the function of ECFCs extracted from a neonatal rat model mimicking BPD. Following 2 weeks of

exposure of neonatal rats to hyperoxia (95% O<sub>2</sub>), the lungs of newborn rats develop a consistent and irreversible histological pattern of alveolar simplification and vascular paucity, characteristic of human BPD (Figure 3A).

When plated at equal densities and cultured in identical conditions, rat lung ECFCs from the hyperoxia-exposed rats showed reduced cell growth (Figure 3B).

ECFCs from hyperoxia-exposed rat lungs formed fewer cordlike endothelial networks in comparison with

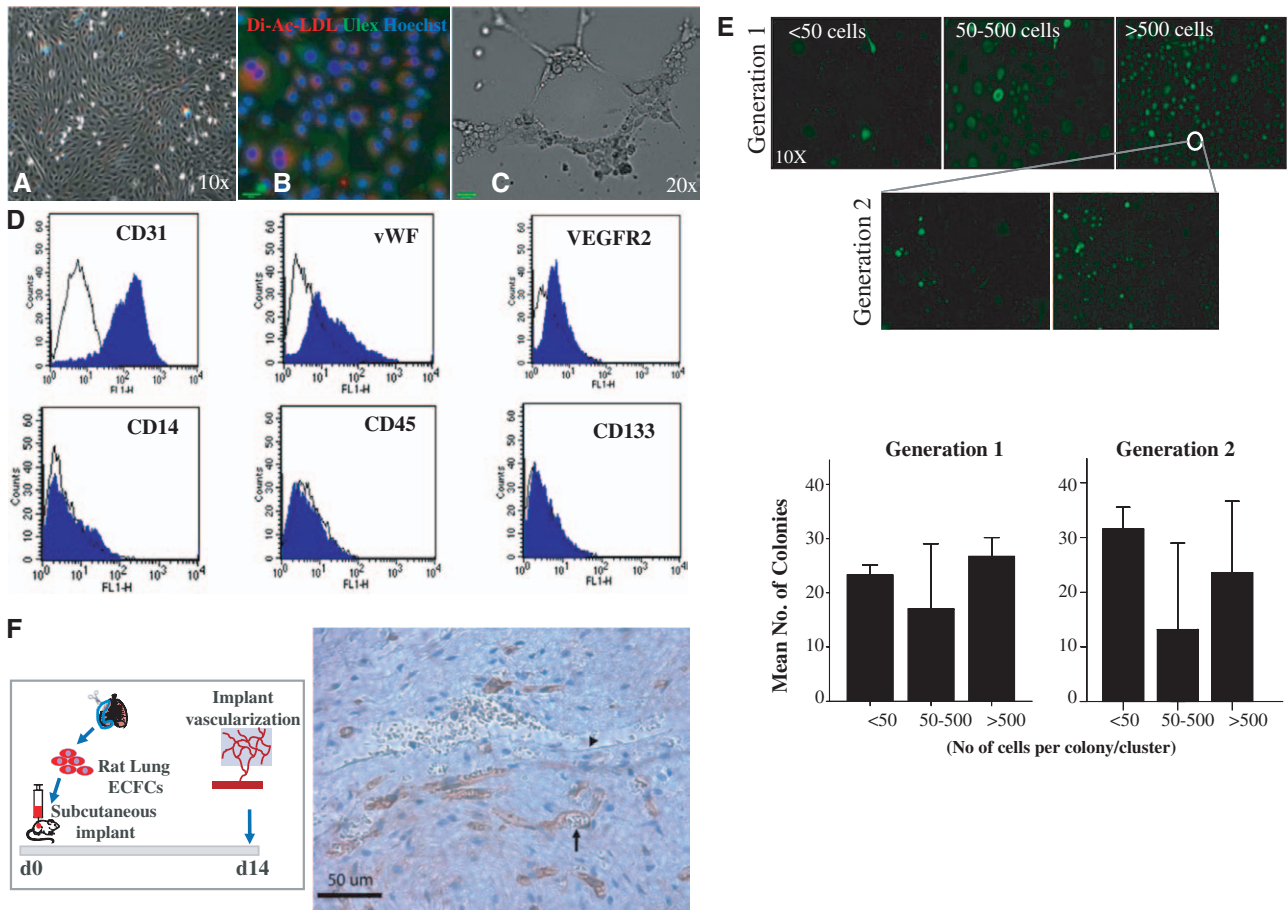


**Figure 2.** ECFCs exist in the developing rat lung. **A**, Phase-contrast microscopy showing characteristic cobblestone-like colonies of CD31-positive cells obtained by beads isolation. **B**, These cells demonstrate Dil-acLDL uptake (red) within 4 hours of incubation and *Ulex europaeus*-lectin binding (green) within 1 hour of incubation after fixation. Counterstaining with Hoechst 33258 (blue) illustrates that all adherent cells are positive for LDL uptake and *U. europaeus* (Ulex)-lectin binding. **C**, These cells form tube-like structures when suspended in Matrigel. **D**, Fluorescent-activated cell sorting. Isolated endothelial cells are positive for endothelial-specific cell surface antigens CD31, vWF, and VEGFR2 and negative for monocyte/macrophage-specific CD14 and hematopoietic cell-specific CD45 and CD133. **E**, Single-cell clonogenic assay. Rat lung endothelial cells are capable of giving rise to clusters (up to 50 cells) or colonies 50 to 500 cells (low proliferative potential, LPP) or >500 cells (high proliferative potential, HPP) in 96-well plates when plated at a seeding density of 1 cell per well. Results represent the mean±standard error of mean of 3 independent experiments. On replating, HPP ECFCs were able to form clusters or secondary colonies with LPP and HPP. **F**, Subcutaneous Matrigel Plug Assay. Rat lung ECFCs form blood vessels de novo when seeded on fibronectin-collagen plugs ( $10^6$  ECFCs per implant) and implanted subcutaneously into the flanks of NOD/SCID mice. Fourteen days postimplantation, the cellularized implants were excised, paraffin embedded, and stained with hematoxylin and eosin and anti-human CD31 (brown). The arrow points to a rat endothelial cell; the rat endothelial cell lines a vessel filled with mouse red blood cells indicating that the rat endothelial cells have connected with the mouse circulation. The arrowhead points to a murine endothelial cell lining a mouse blood vessel. Dil-acLDL indicates Dil-acetylated low-density lipoprotein; ECFC, endothelial colony-forming cell; LDL, low-density lipoprotein; and NOD/SCID, nonobese diabetic/severe combined immunodeficiency.

controls as assessed by total cord length by  $32.7\pm 11.8\%$  ( $P<0.05$ ) and number of intersects by  $48.2\pm 5.3\%$  ( $P<0.05$ ; Figure 3C).

In single-cell clonogenic assays,  $23.6\pm 2.5\%$  of single plated ECFCs from the control group versus only  $9.3\pm 3.2\%$  of ECFCs from the hyperoxia group were capable of forming HPP colonies containing >500 cells each ( $P<0.05$ ; Figure 3D). No significant difference between the groups was observed in the percentage of cells that formed low proliferative potential colonies containing <50 cells or 50 to 500 cells.

Together, these findings suggest a functional deficiency in the ECFCs isolated from lungs of hyperoxia-exposed newborn rats. Because angiogenesis contributes to normal

alveolarization and oxygen-induced arrested alveolarization is associated with decreased ECFC function, we investigated the therapeutic potential of human cord blood-derived ECFCs to restore normal alveolarization in this model.

### Human Cord Blood-Derived ECFCs Reverse Alveolar Growth Arrest, Preserve Lung Vasculature, and Attenuate Pulmonary Hypertension in Hyperoxia-Induced BPD in Newborn Rodents

Exposure of newborn *rag<sup>-/-</sup>* mice to hyperoxia (85%  $O_2$ ) from P4 to P14 (Figure 4A) increased lung compliance (Figure 4B) and induced a histological pattern reminiscent of human BPD, characterized by fewer, enlarged alveolar structures (mean

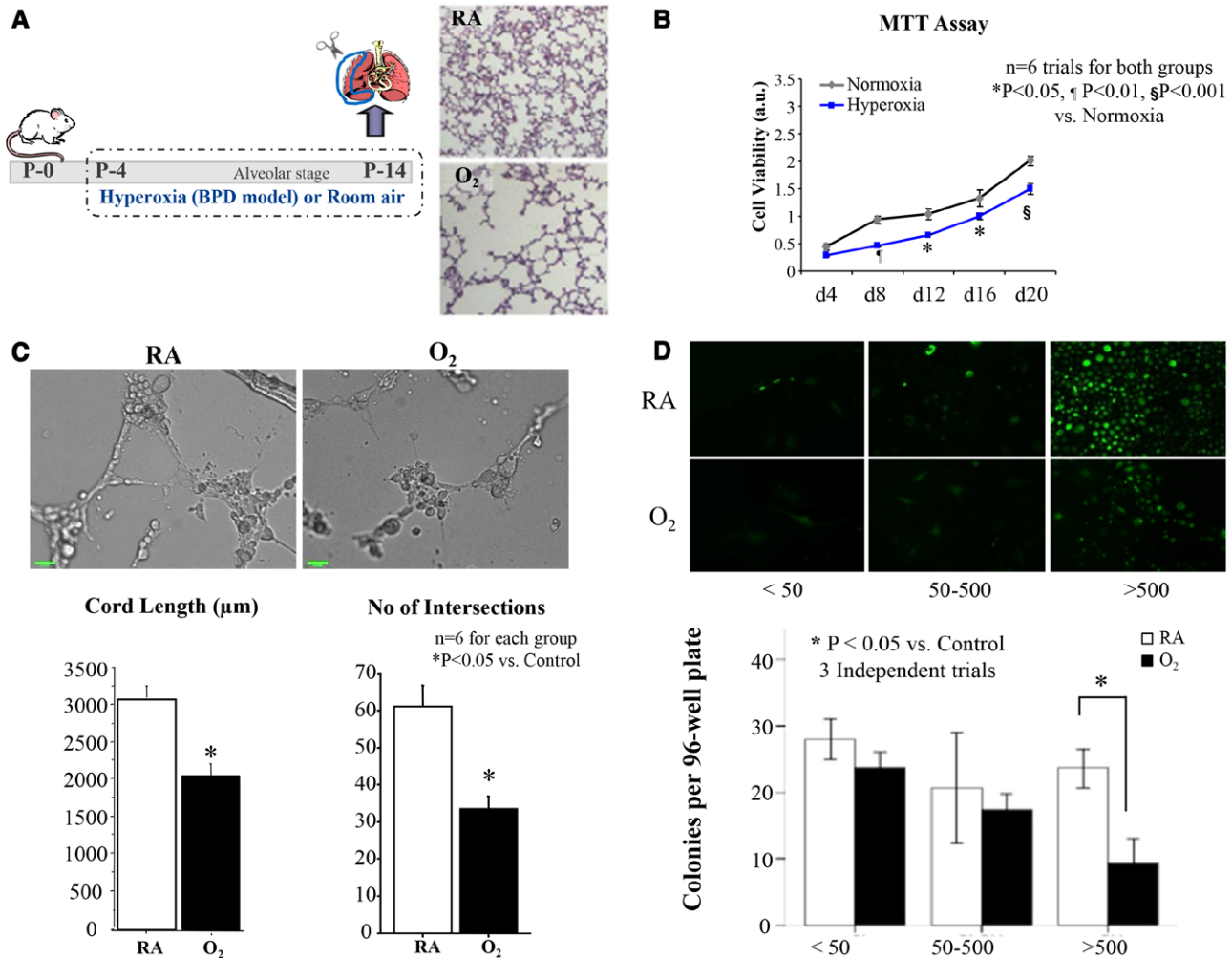


**Figure 3.** Rat lung ECFC function is perturbed in hyperoxia-induced experimental BPD in newborn rats. **A**, Schematic describing the rat model of hyperoxia-induced BPD. Newborn rats are housed in 95% O<sub>2</sub> from postnatal day (P) 4 to P14 and studied in comparison with room air (RA)-raised control rats. Exposure of rat pups to hyperoxia during the alveolar stage of lung development results in arrested alveolar growth characterized by larger and fewer alveolar structures as shown in hematoxylin and eosin-stained representative lung slides. ECFCs were isolated from RA and hyperoxia-exposed rat lungs on P14, and their proliferative, clonogenic, and vessel-forming potentials were assessed. **B**, MTT Assay. Lung ECFCs from RA and hyperoxic animals were plated at equal cell densities and cultured under identical culture conditions. ECFCs from the hyperoxia-exposed group showed decreased cell growth as assessed by MTT assay (n=6, *P*<0.05 on days 12 and 16, *P*<0.01 on day 8, and *P*<0.001 on day 20). **C**, Matrigel assay. Quantitative assessment of the ability to form tube-like structures on Matrigel reveals a significant decrease in the total cord length and the number of intersects in the hyperoxia-exposed ECFCs in comparison with RA ECFCs (n=6 for each group, \**P*<0.05). **D**, Comparative single-cell assay. Colony-forming potential of single-cell-plated rat lung ECFCs was assessed by measuring the percentage of single ECFCs capable of generating colonies after 14 days in culture. Significantly fewer ECFCs from the hyperoxia group are capable of generating colonies with ≥500 cells in comparison with RA controls (n=6 lungs/group, \**P*<0.05). BPD indicates bronchopulmonary dysplasia; ECFC, endothelial colony-forming cell; and MTT, 3-(4,5-dimethylthiazol-2-yl)-2,5-diphenyl tetrazolium bromide.

linear intercept  $41 \pm 2.3$  versus  $25.6 \pm 1.9$  in room-air controls, *P*<0.05; Figure 4C and 4D). Intrajugular administration of cord blood-derived ECFCs at P14 after established alveolar growth arrest, significantly improved lung compliance (Figure 4B) and alveolar architecture (mean linear intercept  $30.3 \pm 1.6$ , *P*<0.05; Figure 4C and 4D). ECFCs had no adverse effect on lung function and structure in room air-housed control animals.

Hyperoxia-exposed mice had decreased lung vascular growth (mean number of blood vessels/high power field  $3.5 \pm 0.3$  versus  $2.2 \pm 0.4$ ; Figure 5A and 5B) and exhibited pulmonary hypertension as assessed by echo Doppler (PAAT  $11.4 \pm 0.4$  versus  $14.9 \pm 1.6$  in room-air controls, *P*<0.05) and right ventricle hypertrophy (right ventricle/left ventricle plus

septum ratio  $0.35 \pm 0.05$  versus  $0.22 \pm 0.06$  in room-air controls, *P*<0.01; Figure 5C). ECFC therapy restored PAAT almost to control levels ( $14.1 \pm 2$ ) and significantly reduced right ventricle hypertrophy (right ventricle/left ventricle plus septum ratio  $0.26 \pm 0.03$ ; Figure 5D).

Similarly, ECFC therapy restored normal alveolar architecture (Figure 1A in the online-only Data Supplement), lung vascular growth (Figure 1B in the online-only Data Supplement) in newborn RNU rats that were exposed to 95% hyperoxia from P4 to P14 (immunocompromised rat BPD model). In addition, ECFC therapy significantly attenuated right ventricle hypertrophy in hyperoxia-exposed RNU rats (Figure 1D in the online-only Data Supplement).



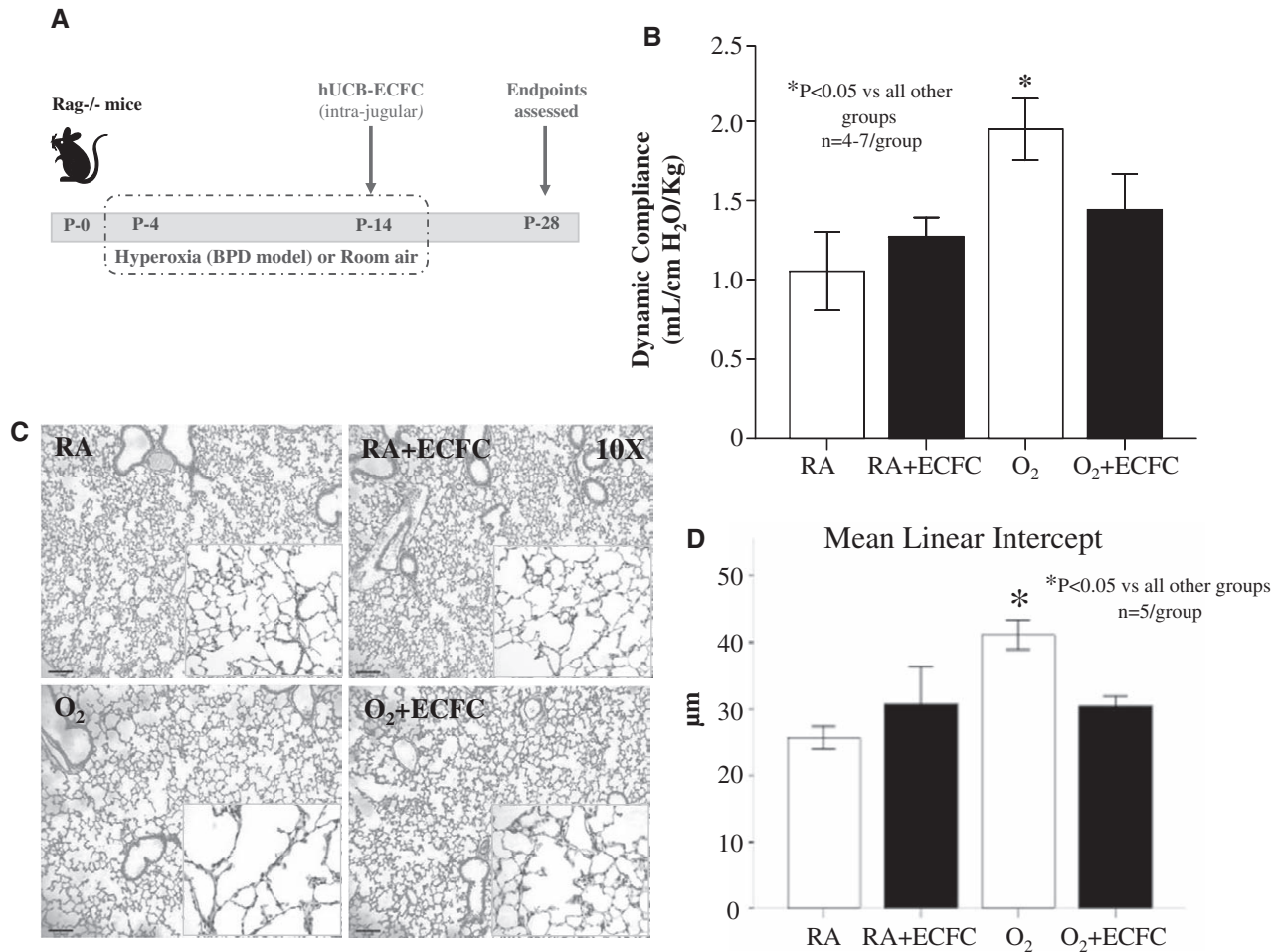


**Figure 4.** Human umbilical cord blood ECFC therapy improves lung function and reverses alveolar growth arrest in hyperoxia-exposed newborn mice. **A**, Experimental design. Newborn *rag*<sup>-/-</sup> mice were housed in room air (RA) or 85% O<sub>2</sub> from postnatal day (P) 4 to P14. At P14, mice were treated with intrajugular injections of human umbilical cord blood–derived ECFCs and housed in RA until the assessment of end points on P28. **B**, Lung function testing. Untreated mice exposed to hyperoxia had significantly increased lung compliance in comparison with RA and ECFC-treated RA controls ( $n=4-7$ ,  $P<0.05$ ). Lung compliance was significantly improved in hyperoxia-exposed mice treated with ECFCs in comparison with untreated hyperoxia-exposed controls ( $P<0.05$ ). **C**, Representative hematoxylin and eosin–stained lung sections showing larger and fewer alveoli in untreated hyperoxia-exposed (O<sub>2</sub>) lungs in comparison with control mice housed in RA at P28. Intrajugular administration of ECFCs in O<sub>2</sub>-exposed animals preserved alveolar growth. ECFCs did not affect lung structure in control RA mice. **D**, Quantitative assessment of alveolar architecture by mean linear intercept confirms the protective effect of ECFCs on alveolar growth ( $n=5$ /group,  $*P<0.05$ ). BPD indicates bronchopulmonary dysplasia; ECFC, endothelial colony-forming cell; and hUCB, human umbilical cord blood.

### ECFC Engraftment and Contribution to Lung Neovascularization

Quantification of human ECFCs by the use of quantitative reverse transcriptase–polymerase chain reaction showed a low rate of engraftment in recipient lungs with a drastic decrease in detected human Alu sequences from the first day after injection to almost undetectable levels within 3 days (Figure 6A). Fourteen days after fluorescent-labeled ECFC administration, very few cells were found in the lung (Figure 6B). However, when lung ECFCs were isolated from RNU rats and tested for clonogenic capacity, resident lung ECFCs from the treated hyperoxia group were capable of forming significantly more HPP colonies than the untreated hyperoxia-exposed group ( $P<0.05$ ; Figure IIA in the online-only Data Supplement). In addition, lung ECFCs from the treated animals formed more extensive endothelial networks than the untreated animals in the hyperoxia group as assessed by cord length and number

of intersects ( $P<0.05$ ; Figure IIB in the online-only Data Supplement).

### Paracrine Effect of Human Cord Blood–Derived ECFCs

Given the low engraftment of ECFCs at the doses administered in these studies and evidence that some endothelial progenitor cells (EPCs) secrete factors that promote tissue repair,<sup>18</sup> we hypothesized that ECFCs may also exert a paracrine activity that mediates the reparative response in the lung. To verify this, we assessed the effect of cell-free human cord blood–derived ECFC CdM *in vitro* and *in vivo*.

*In vitro*, we assessed the protective effects of ECFC–CdM by using 2 experimental models representing the epithelial and endothelial compartments of lung alveoli. First, confluent monolayers of AT2 cells were subject to a pipette tip–inflicted scratch injury in the presence of DMEM,

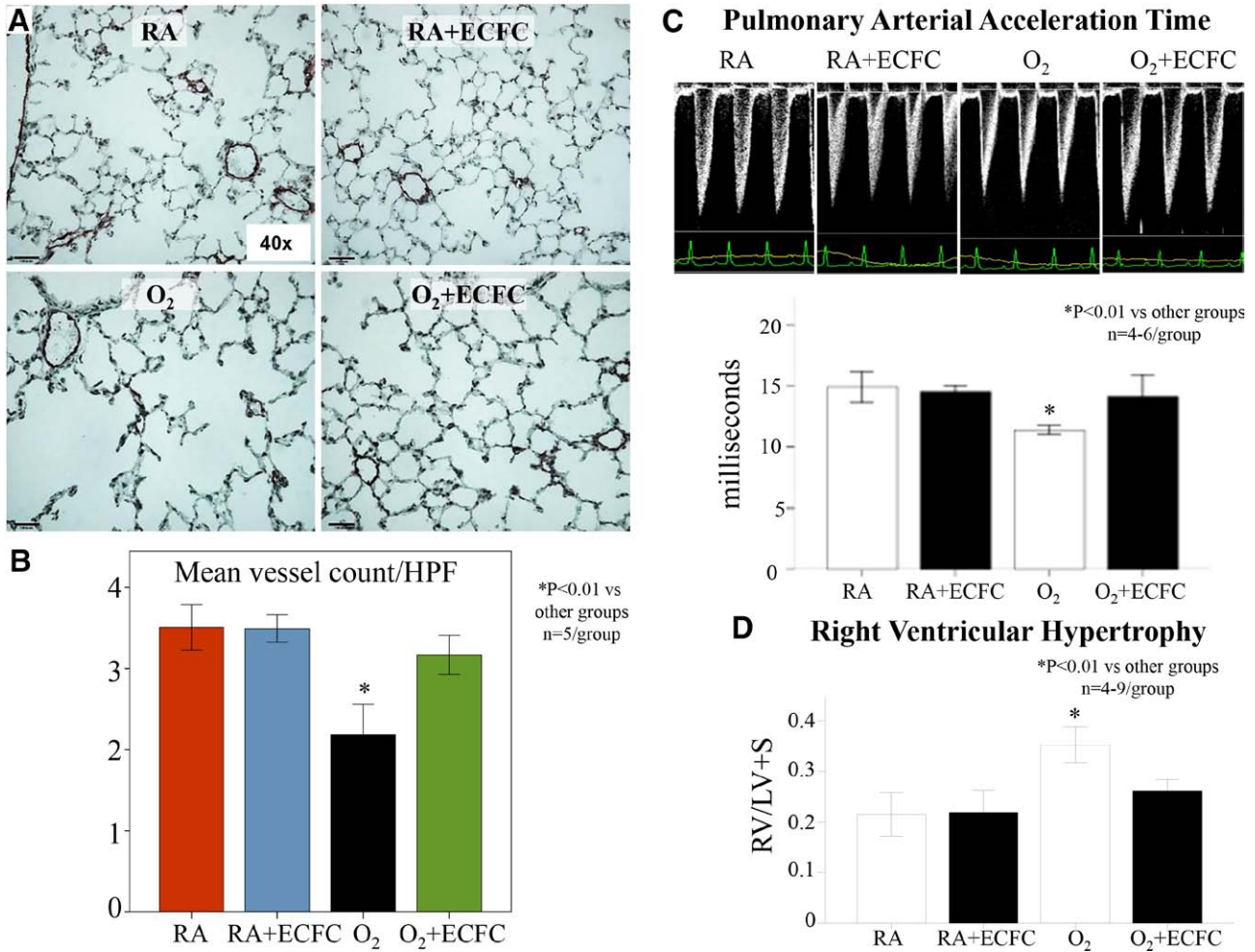


**Figure 5.** Human umbilical cord ECFCs improve lung angiogenesis and prevent pulmonary hypertension in hyperoxia-exposed newborn mice. **A** and **B**, Effects of ECFC treatment on pulmonary vessel density assessed on lung slides stained with von Willebrand Factor at P28. The pulmonary vessel density of 30 to 100µm sized blood vessels per 10 high-power fields (×40) was significantly decreased in the lungs of O<sub>2</sub>-exposed animals in comparison with RA. Intrajugular injection of ECFCs significantly improved pulmonary vessel density (n=5/group, \*P<0.01). **C**, Pulmonary arterial acceleration time (PAAT) was significantly decreased in O<sub>2</sub>-exposed animals in comparison with controls. Intrajugular ECFCs restored the PAAT almost to control levels (n=4–6/group, \*P<0.01). **D**, Hyperoxia-exposed mice had significant RVH as indicated by the increase in right ventricle/left ventricle plus septum (RV/LV+S) ratio in comparison with controls. ECFC therapy significantly reduced RVH (n=4–9/group, \*P<0.01). ECFC indicates endothelial colony-forming cell; HPF, high-power field; RA, room air; and RVH, right ventricle hypertrophy.

HUVEC-CdM, or ECFC-CdM. At 12 hours, AT2 cell wound closure was significantly higher with ECFC-CdM than with DMEM and HUVEC-CdM (Figure 7A and 7B). Second, human fetal lung ECFCs were suspended in

serum-free Matrigel overlaid with DMEM, HUVEC-CdM, or ECFC-CdM and incubated in room air or 95% oxygen. At 6 hours, hyperoxia significantly decreased endothelial cord-like structure formation in DMEM and HUVEC-CdM,

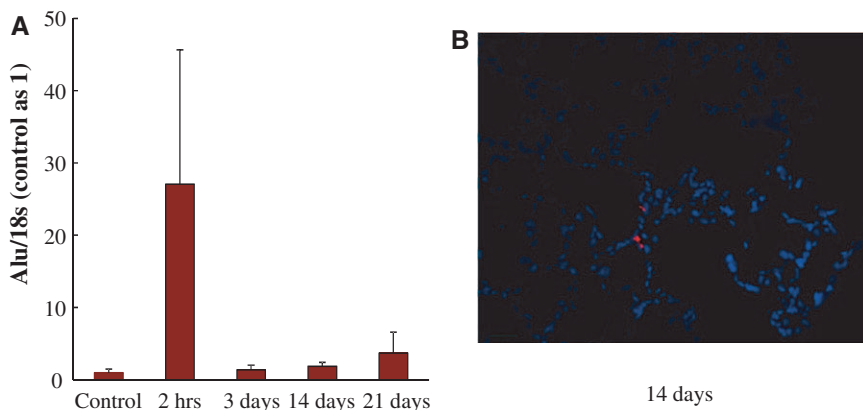


**Figure 6.** Low engraftment rate after intrajugular injection of human umbilical cord ECFCs. **A**, Quantitative RT-PCR for human Alu sequences in the lung revealed a rapid decline during the first day after injection. Human DNA became almost undetectable 3 days after injection. **B**, Representative frozen lung section at P21 depicting rare fluorescently labeled ECFCs. ECFC indicates endothelial colony-forming cell; and RT-PCR, reverse transcriptase-polymerase chain reaction.



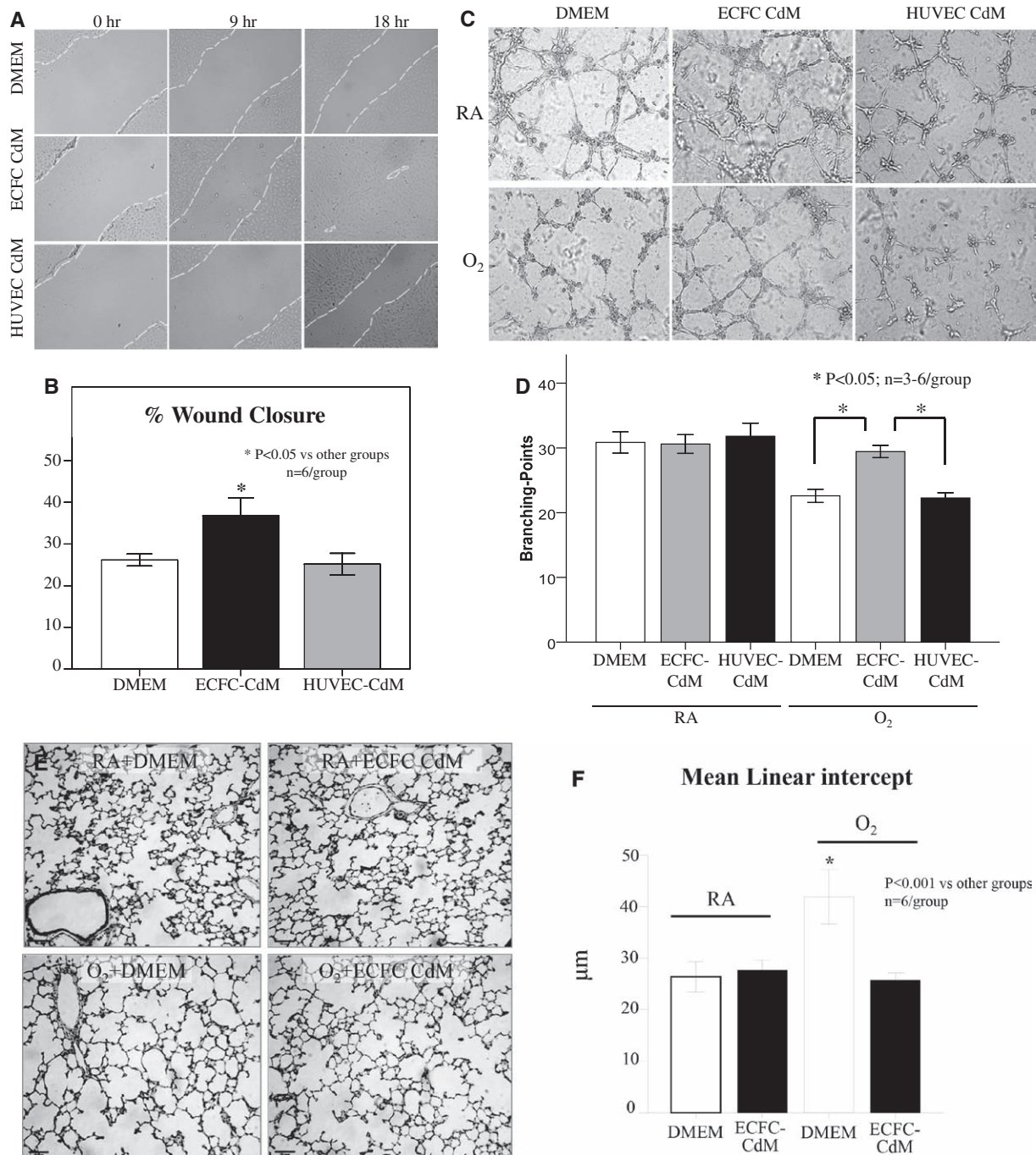


**Figure 7.** Paracrine effect of human umbilical cord ECFCs. **A**, Representative confluent monolayers of freshly isolated rat alveolar type 2 epithelial cells (AT2) damaged by the use of a pipette tip, washed to remove damaged cells, and treated with DMEM, ECFC-derived conditioned medium (CdM) or HUVEC CdM. **B**, The percentage of wound closure showed that ECFC CdM accelerated AT2 wound closure in comparison with DMEM and HUVEC CdM (n=6/group, \*P<0.05). **C**, Representative endothelial network formation assay on Matrigel of human fetal lung ECFCs treated with DMEM, ECFC-derived CdM or HUVEC CdM in room air (RA) and hyperoxia (O<sub>2</sub>). **D**, Quantitative assessment of cordlike structure formation shows a significant decrease in the number of intersects in hyperoxia in DMEM and HUVEC CdM-treated ECFCs in comparison with RA-exposed ECFC. ECFC CdM preserved the number of intersects in hyperoxia (n=3–6/group, \*P<0.05). **E**, Representative hematoxylin and eosin section showing arrested alveolar growth in O<sub>2</sub>-exposed newborn rats in comparison with RA controls. ECFC CdM significantly preserved alveolar growth in O<sub>2</sub>-exposed newborn rats in comparison with RA controls. **F**, Quantitative assessment of the mean linear intercept confirms the protective effect of ECFC CdM on alveolar growth (n=6/group, \*P<0.001). **G**, Mean data showing decreased pulmonary vessel density in O<sub>2</sub>-exposed newborn rats in comparison with RA controls as assessed by the number of barium-filled pulmonary vessels. ECFC CdM significantly attenuated the loss of pulmonary vessels in hyperoxia (n=5/group, \*P<0.01). **H**, Pulmonary arterial acceleration time (PAAT) was significantly decreased in O<sub>2</sub>-exposed animals in comparison with controls. ECFC CdM preserved the PAAT in comparison with untreated O<sub>2</sub>-exposed animals (n=5–6/group, \*P<0.05). **I**, Hyperoxia-exposed rats had significant RVH as indicated by the increase in right ventricle/left ventricle plus septum (RV/LV+S) ratio in comparison with controls. ECFC CdM significantly reduced RVH in comparison with untreated O<sub>2</sub>-exposed animals (n=5–6/group, \*P<0.05). DMEM indicates Dulbecco's modified Eagle medium; ECFC, endothelial colony-forming cell; HUVEC, human umbilical endothelial cell; and RVH, right ventricle hypertrophy.

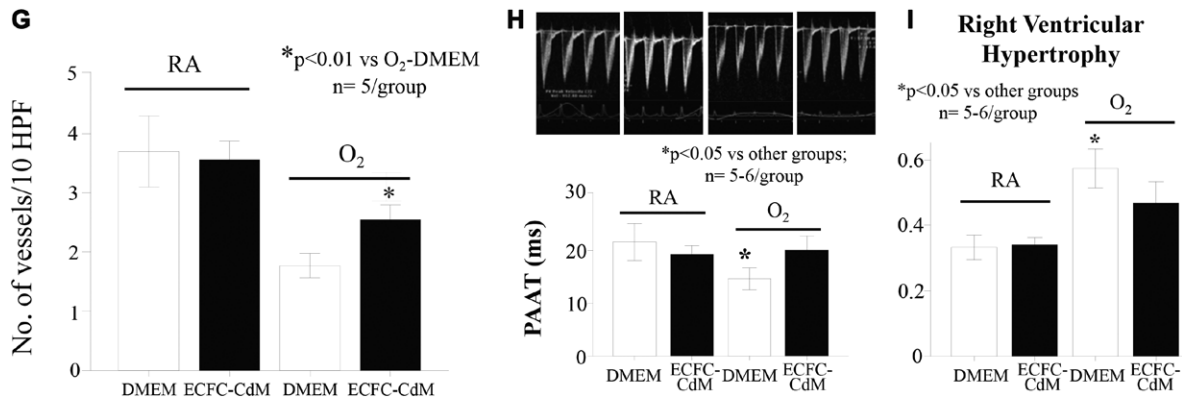


Figure 7. Continued.

whereas ECFC-CdM significantly preserved ECFC network formation (Figure 7C and 7D).

In vivo, ECFC-CdM was administered as daily intraperitoneal injections from P4 to P21 to neonatal rats exposed to hyperoxia. CdM therapy preserved alveolar growth (Figure 7E and 7F), lung vascular growth (Figure 7G), and attenuated pulmonary hypertension as assessed by the PAAT and right ventricular hypertrophy (Figure 7H and 7I). ECFC-CdM had no adverse effects on lung structure and lung vascularity in room-air control animals.

### Long-Term Effects of ECFC Therapy

Intrajugular delivery of ECFCs at P14 appeared safe and efficient up to 10 months of life. Air spaces remained enlarged (Figure 8A and 8B), and exercise capacity (Figure 8C) and PAAT (Figure 8D) remained perturbed in hyperoxic-exposed animals in comparison with room-air controls. In contrast, hyperoxic-exposed neonatal mice that had received ECFCs in the neonatal period exhibited preserved alveolar architecture (Figure 8A and 8B), significantly improved exercise capacity (Figure 8C) and PAAT (Figure 8D) at 10 months of age. Control room air-housed animals treated with ECFCs showed no alterations in any of these parameters. Other organs including the brain, heart, liver, kidney, and spleen had no signs of impaired architecture (data not shown).

### Discussion

Here, we show that the developing human and rat lung harbors resident ECFCs capable of self-renewal and de novo vessel formation in vivo. We also provide evidence that hyperoxia perturbs human and rat lung ECFC function in vitro and in vivo in experimental oxygen-induced BPD, respectively. Furthermore, exogenous, human cord blood-derived ECFCs restore normal lung alveolar and vascular growth and function, diminish pulmonary hypertension, and restore resident lung ECFC function in this model in comparison with control animals. This effect is mediated through a paracrine effect. The therapeutic benefit persisted at 10 months with no adverse effects on lung structure and exercise capacity in hyperoxia-exposed animals.

Increasing evidence suggests that blood vessels contribute to normal lung growth as opposed to passively following the development of the airways.<sup>5</sup> This has led to the current working hypothesis that the preservation of vascular growth and endothelial survival promotes alveolar growth and

sustains the architecture of the alveoli. The consistent association between arrested alveolar development and impaired capillary formation in human and experimental BPD and the demonstration that angiogenic growth factors promote normal alveolar development and repair further support this finding. Thus, if angiogenic growth factors and adequate lung vascularization contribute to lung development and integrity, then circulating or resident ECFCs are appealing candidate cells likely to be involved in the same mechanisms. The isolation of a circulating cell that gives rise to cells appearing endothelial-like in vitro and with the potential to incorporate at sites of neovascularization in vivo by Asahara et al<sup>19</sup> challenged the paradigm that vasculogenesis is a process restricted to embryonic development and opened exciting new therapeutic avenues. A current limitation is the ability to define an EPC based on a set of markers that can unambiguously identify this cell type. To date, at least 3 different methodologies exist for the isolation of EPCs. Schematically, EPCs appear to represent 2 distinct cell populations: the minimally proliferative but proangiogenic hematopoietic or macrophage-like phenotype (that includes circulating angiogenic cells and colony-forming unit Hill colonies) and the highly proliferative nonhematopoietic phenotype (ECFCs).<sup>12</sup> Based on their timing of emergence in culture, these populations have also been described as early- and late-outgrowth EPCs, respectively.<sup>20</sup> ECFCs, which are phenotypically indistinguishable from cultured endothelial cells, demonstrate high proliferative potential and the capacity for self-renewal and de novo vessel formation.<sup>21,22</sup> ECFCs reside throughout the vascular endothelium contributing to vascular integrity and are mobilized into a circulating pool of endothelial progenitors, putatively involved in neovascularization via tissue recruitment and homing.<sup>21</sup> Recently, Alvarez et al<sup>9</sup> described a population of resident pulmonary microvascular EPCs in adult rat lungs that display a high proliferative potential and are capable of de novo angiogenesis in vivo. These cells resemble the ECFCs previously isolated from the peripheral circulation and in human umbilical cord blood. Similar cells have now been described in the mouse<sup>23</sup> pulmonary circulation. This suggests that ECFCs could be the primary progenitor population participating in neovascularization in the lung. The existence of these resident lung ECFCs in the developing lung and their role in arrested alveolar growth in BPD is unknown. We reasoned that ECFCs dysfunction could



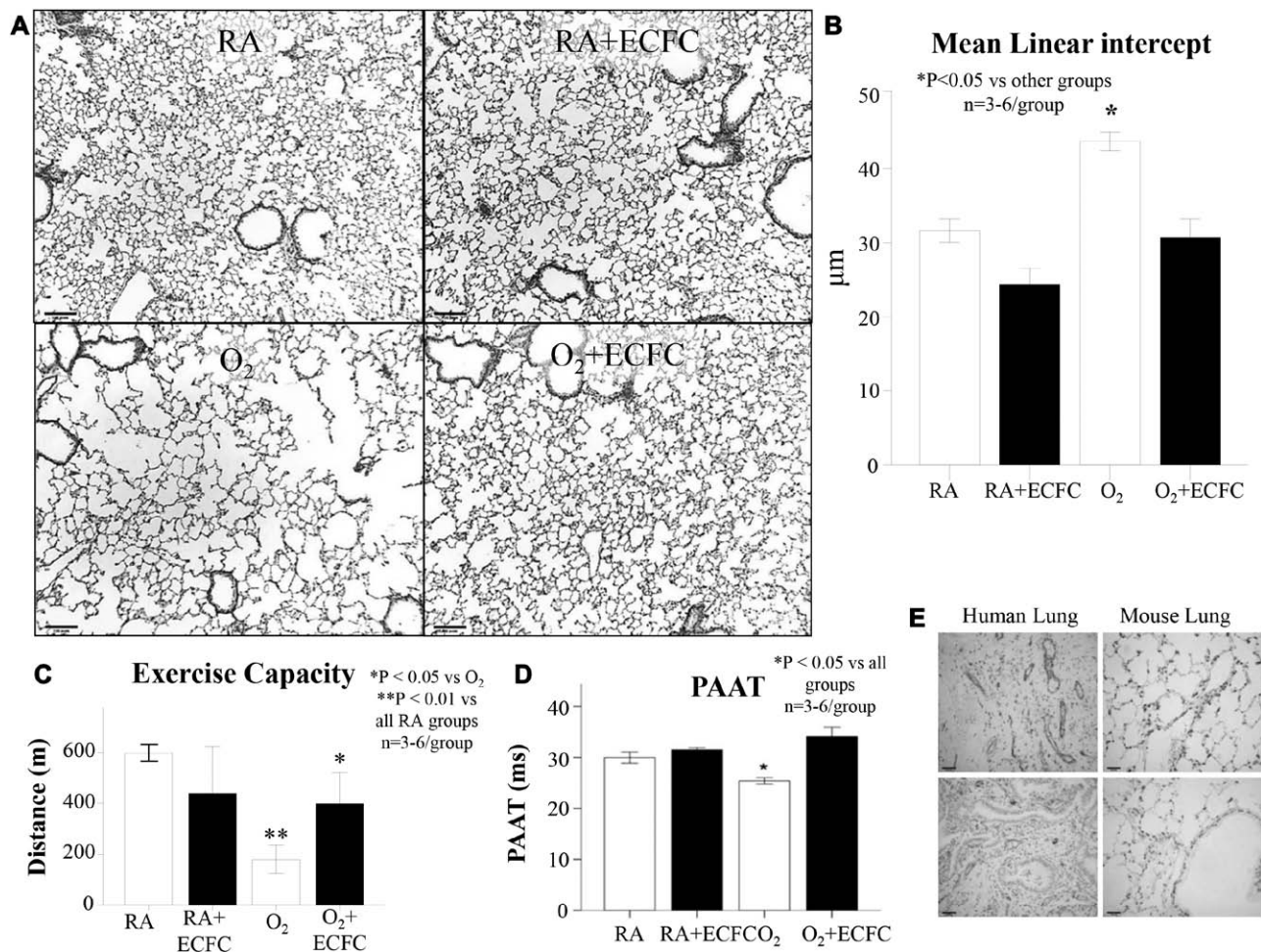


**Figure 8.** Long-term safety and efficacy of ECFC cell therapy. **A**, Representative hematoxylin and eosin–stained lung sections at 10 months of age shows persistent alveolar simplification in hyperoxia-exposed animals in comparison with lungs from rats housed in room air (RA). Oxygen-exposed animals treated with ECFCs have improved lung histology. **B**, The mean linear intercept confirms arrested alveolar growth in untreated O<sub>2</sub>-exposed animals in comparison with RA and RA+ECFC-treated animals and preserved alveolar structure with ECFC therapy in comparison with untreated O<sub>2</sub>-exposed animals ( $n=3-6/\text{group}$ ,  $*P<0.05$ ). **C**, Oxygen-exposed animals experienced reduced exercise capacity in comparison with RA-housed animals. Oxygen-exposed animals treated with ECFC had improved exercise capacity ( $n=3-6$  animals/group,  $*P<0.05$ ). **D**, Oxygen-exposed animals had decreased pulmonary arterial acceleration time (PAAT) in comparison with RA and RA+ECFC animals. Oxygen-exposed animals treated with ECFC had improved PAAT in comparison with untreated O<sub>2</sub>-exposed animals ( $n=3-6$  animals/group,  $*P<0.05$ ). **E**, Representative lung section of an ECFC-treated mouse lung at 10 months of age showing no presence of CD31-positive structures. In contrast, CD31 staining is abundant in a human adult lung. ECFC indicates endothelial colony-forming cell.

underlie the pathogenesis of diseases such as BPD, characterized by disrupted vascular growth.

We adopted a procedure based on the already existing protocol for recovering circulating ECFCs from bone marrow or peripheral blood<sup>10</sup> to demonstrate the presence of resident ECFCs in fetal human and neonatal rat lung. These cells displayed the stringent characteristics of ECFCs including (1) the ability to generate colonies with  $\geq 500$  daughter cells derived from cultured single cells and (2) some of the clonogenic cells are capable of self-renewal, and (3) the capacity to form vessels de novo, when impregnated in collagen-fibronectin gels and implanted subcutaneously in recipient immunodeficient mice.

Given the importance of angiogenesis in normal alveolar growth, we hypothesized that ECFC function would be impaired in disease conditions associated with arrested alveolar growth such as BPD. Earlier observations reported

on the susceptibility of cord blood–derived ECFCs to oxidant damage.<sup>24</sup> Furthermore, cord blood–derived ECFCs are lower in number in preterm infants who subsequently develop BPD versus those who do not develop BPD.<sup>25,26</sup> Here, we show that resident human lung ECFCs exposed to hyperoxia in vitro and rat ECFCs isolated from the lung of a hyperoxia-induced BPD model that display arrested alveolar growth were significantly hampered in their ability to proliferate, form vascular networks in vitro, and generate colonies with HPP in comparison with ECFCs isolated from control lungs. Although there are no specific cell surface markers to identify the resident ECFC within the vascular endothelial intima in vivo, it is interesting that endothelial replacement or expansion within the aorta has long been known to emerge within clusters of endothelial cells rather than a dispersed pattern during normal embryonic growth or in animals with hypertension.<sup>27,28</sup> Confirmation of the ECFC



within the vascular endothelial intima will require further work to identify a unique and specific marker.

These data formed the rationale for testing the therapeutic potential of umbilical cord blood–derived ECFC supplementation in experimental BPD. Here, we provide the first evidence for the therapeutic benefit of ECFCs in restoring lung vascular and alveolar growth and lung function, as well, in an established model of BPD. ECFCs also attenuated pulmonary hypertension, a complication commonly associated with severe BPD. In addition, treatment with cord blood–derived ECFCs restored colony-forming and capillary-like network-forming capabilities of resident lung ECFCs of newborn rats with experimental BPD. These data are consistent with the beneficial effect of angiogenic factors in experimental BPD<sup>29–31</sup> and underscore the therapeutic benefit of promoting lung angiogenesis to repair the lung. Altogether, these observations suggest an increased susceptibility of ECFCs in the developing lung to hyperoxia that may contribute to impaired lung vascular and alveolar growth in BPD and that ECFC supplementation represents a promising strategy for lung repair.

In this study, we have used ECFCs derived from human cord blood to document the therapeutic effect of these cells in a model of impaired lung development. This clinically relevant source of ECFCs appears particularly appealing for treating neonatal diseases. To test ECFCs of human origin we used immunodeficient *rag<sup>-/-</sup>* mice, in which hyperoxia-mediated lung injury appeared less pronounced. Practical constraints in obtaining ECFCs from the rat cord blood limited us from using the more robust model of in newborn Sprague-Dawley rats. Despite this limitation, the demonstrated findings are consistent and convincing with regard to the therapeutic effect of ECFCs in BPD.

In this study, we administered ECFCs after established arrested alveolar growth and after hyperoxic exposure. The rationale was based on previous *in vitro* studies suggesting that hyperoxia impairs cord blood–derived ECFC function.<sup>24,32</sup>

Lung injury in neonatal mice exposed to hyperoxia is also associated with decreased early-outgrowth EPCs<sup>33</sup> and can be overcome by bone marrow–derived angiogenic cell infusion.<sup>34</sup> Further evidence for the role of EPCs in lung repair is provided by experimental and clinical data showing that (1) bone marrow–derived EPCs attenuate lipopolysaccharide-induced acute lung injury<sup>35</sup> and elastase-induced emphysema,<sup>36,37</sup> (2) EPCs are higher in patients with acute lung injury than in healthy control subjects,<sup>38</sup> and (3) the increase in circulating EPCs correlates with improved outcome and illness severity and improved survival in acute<sup>38,39</sup> and chronic<sup>40</sup> lung disease, suggesting a prognostic role similar to ischemic heart disease.

Very few engrafted cells were detected by immunofluorescence and analysis of human-specific Alu sequences. We did not pursue a dose-dependent study to find a concentration of ECFC that engrafted into regenerating vasculature in this model. Others have noted that human ECFCs can form up to 27% of the vascular endothelium in recovering ischemic muscle tissue of nude mice subjected to a hind limb ischemic injury.<sup>41</sup> Additional work may determine that higher doses of administered human cells may lead to sustained engraftment.

Alternatively, this observation may suggest that, similar to other cell-based strategies including early outgrowth EPCs and mesenchymal stromal cell therapy, ECFCs exert their therapeutic benefit mainly through a paracrine activity. This paracrine activity is supported by the protective effect of cell-free ECFC-derived CdM on alveolar epithelial cell wound healing and human lung ECFC vascular network formation *in vitro*. As well, *in vivo*, ECFC-derived CdM restored alveolar and lung vascular growth comparable to whole-cell therapy.

In our *in vivo* studies, CdM was administered as daily intraperitoneal injections from P4 to P21 with the reasoning that repeated dispensation would be necessary to ensure continuous availability of protective factors. With cell therapy, on the other hand, we expected a more sustained release of protective factors from the transfused cells even after a single intravenous dose. However, recent observations suggest that a single injection of CdM may be sufficient to prevent oxygen-induced lung injury in neonatal mice.<sup>1,2</sup> The biologically active component of mesenchymal stromal cell-derived CdM seems to be contained in exosomes, membrane-derived nanoparticles, as recently demonstrated in a hypoxia-induced model of pulmonary hypertension.<sup>42</sup> It is likely that ECFCs, as many other cells, produce exosomes. Whether these exosomes can be used as biomarkers or therapeutic tools remains to be studied.

A concern with cell-based therapy, especially in the neonate, is the risk of long-term adverse effects including tumor formation. Here, we show that the therapeutic benefit in the ECFC-treated mice was still present at 10 months of age without adverse effects on lung structure or exercise capacity. No tumors were detectable by examining serial histological sections of major organs including the lung, brain, heart, liver, kidney, and spleen at 10 months post-ECFC injection.

In conclusion, we show for the first time that ECFCs exist in the distal vasculature of the developing mammalian lung, and their functional capacity is impaired in oxygen-induced lung damage. We also show that therapeutic supplementation with human umbilical cord blood–derived ECFCs is feasible, efficacious, and apparently safe in this experimental O<sub>2</sub>-induced model of BPD in neonatal mice.

## Sources of Funding

This work was supported by a grant from the Canadian Institutes for Health Research (CIHR; to Dr Thébaud) and the Riley Children's Foundation (Dr Yoder). Dr Alphonse was the recipient of an Alberta Innovate Health Solutions (AIHS) stipend. Dr Thébaud was supported by a Canada Research Chair and AIHS clinical investigator award and by the Canadian Foundation for Innovation (CFI).

## Disclosures

None.

## References

1. Goldenberg RL, Culhane JF, Iams JD, Romero R. Epidemiology and causes of preterm birth. *Lancet*. 2008;371:75–84.
2. Mourani PM, Abman SH. Pulmonary vascular disease in bronchopulmonary dysplasia: pulmonary hypertension and beyond. *Curr Opin Pediatr*. 2013;25:329–337.
3. Baraldi E, Filippone M. Chronic lung disease after premature birth. *N Engl J Med*. 2007;357:1946–1955.

4. Wong PM, Lees AN, Louw J, Lee FY, French N, Gain K, Murray CP, Wilson A, Chambers DC. Emphysema in young adult survivors of moderate-to-severe bronchopulmonary dysplasia. *Eur Respir J*. 2008;32:321–328.
5. Thébaud B, Abman SH. Bronchopulmonary dysplasia: where have all the vessels gone? Roles of angiogenic growth factors in chronic lung disease. *Am J Respir Crit Care Med*. 2007;175:978–985.
6. Kunig AM, Balasubramaniam V, Markham NE, Morgan D, Montgomery G, Grover TR, Abman SH. Recombinant human VEGF treatment enhances alveolarization after hyperoxic lung injury in neonatal rats. *Am J Physiol Lung Cell Mol Physiol*. 2005;289:L529–L535.
7. Thébaud B, Ladha F, Michelakis ED, Sawicka M, Thurston G, Eaton F, Hashimoto K, Harry G, Haromy A, Korbitt G, Archer SL. Vascular endothelial growth factor gene therapy increases survival, promotes lung angiogenesis, and prevents alveolar damage in hyperoxia-induced lung injury: evidence that angiogenesis participates in alveolarization. *Circulation*. 2005;112:2477–2486.
8. Ding BS, Nolan DJ, Guo P, Babazadeh AO, Cao Z, Rosenwaks Z, Crystal RG, Simons M, Sato TN, Worgall S, Shido K, Rabbany SY, Rafii S. Endothelial-derived angiocrine signals induce and sustain regenerative lung alveolarization. *Cell*. 2011;147:539–553.
9. Alvarez DF, Huang L, King JA, ElZarrad MK, Yoder MC, Stevens T. Lung microvascular endothelium is enriched with progenitor cells that exhibit vasculogenic capacity. *Am J Physiol Lung Cell Mol Physiol*. 2008;294:L419–L430.
10. Mead LE, Prater D, Yoder MC, Ingram DA. Isolation and characterization of endothelial progenitor cells from human blood. *Curr Protoc Stem Cell Biol*. 2008;chapter 2:unit 2C.1. doi: 10.1002/9780470151808.sc02c01s6.
11. Waszak P, Alphonse R, Vadivel A, Ionescu L, Eaton F, Thébaud B. Preconditioning enhances the paracrine effect of mesenchymal stem cells in preventing oxygen-induced neonatal lung injury in rats. *Stem Cells Dev*. 2012;21:2789–2797.
12. Yoder MC, Mead LE, Prater D, Krier TR, Mroueh KN, Li F, Krasich R, Temm CJ, Prchal JT, Ingram DA. Redefining endothelial progenitor cells via clonal analysis and hematopoietic stem/progenitor cell principals. *Blood*. 2007;109:1801–1809.
13. Ladha F, Bonnet S, Eaton F, Hashimoto K, Korbitt G, Thébaud B. Sildenafil improves alveolar growth and pulmonary hypertension in hyperoxia-induced lung injury. *Am J Respir Crit Care Med*. 2005;172:750–756.
14. Ionescu LI, Alphonse RS, Arizmendi N, Morgan B, Abel M, Eaton F, Duszyk M, Vliagoftis H, Aprahamian TR, Walsh K, Thébaud B. Airway delivery of soluble factors from plastic-adherent bone marrow cells prevents murine asthma. *Am J Respir Cell Mol Biol*. 2012;46:207–216.
15. Pierro M, Ionescu L, Montemurro T, Vadivel A, Weissmann G, Oudit G, Emery D, Bodiga S, Eaton F, Péault B, Mosca F, Lazzari L, Thébaud B. Short-term, long-term and paracrine effect of human umbilical cord-derived stem cells in lung injury prevention and repair in experimental bronchopulmonary dysplasia. *Thorax*. 2013;68:475–484.
16. van Haaften T, Byrne R, Bonnet S, Rochefort GY, Akabutu J, Bouchentouf M, Rey-Parra GJ, Galipeau J, Haromy A, Eaton F, Chen M, Hashimoto K, Abley D, Korbitt G, Archer SL, Thébaud B. Airway delivery of mesenchymal stem cells prevents arrested alveolar growth in neonatal lung injury in rats. *Am J Respir Crit Care Med*. 2009;180:1131–1142.
17. Mund JA, Estes ML, Yoder MC, Ingram DA Jr, Case J. Flow cytometric identification and functional characterization of immature and mature circulating endothelial cells. *Arterioscler Thromb Vasc Biol*. 2012;32:1045–1053.
18. Urbich C, Aicher A, Heeschen C, Dernbach E, Hofmann WK, Zeiher AM, Dimmeler S. Soluble factors released by endothelial progenitor cells promote migration of endothelial cells and cardiac resident progenitor cells. *J Mol Cell Cardiol*. 2005;39:733–742.
19. Asahara T, Murohara T, Sullivan A, Silver M, van der Zee R, Li T, Witzensichler B, Schatteman G, Isner JM. Isolation of putative progenitor endothelial cells for angiogenesis. *Science*. 1997;275:964–967.
20. Yoon CH, Hur J, Park KW, Kim JH, Lee CS, Oh IY, Kim TY, Cho HJ, Kang HJ, Chae IH, Yang HK, Oh BH, Park YB, Kim HS. Synergistic neovascularization by mixed transplantation of early endothelial progenitor cells and late outgrowth endothelial cells: the role of angiogenic cytokines and matrix metalloproteinases. *Circulation*. 2005;112:1618–1627.
21. Ingram DA, Mead LE, Moore DB, Woodard W, Fenoglio A, Yoder MC. Vessel wall-derived endothelial cells rapidly proliferate because they contain a complete hierarchy of endothelial progenitor cells. *Blood*. 2005;105:2783–2786.
22. Ingram DA, Mead LE, Tanaka H, Meade V, Fenoglio A, Mortell K, Pollok K, Ferkowicz MJ, Gilley D, Yoder MC. Identification of a novel hierarchy of endothelial progenitor cells using human peripheral and umbilical cord blood. *Blood*. 2004;104:2752–2760.
23. Schniederermann J, Rennecke M, Buttler K, Richter G, Städtler AM, Norgall S, Badar M, Barleon B, May T, Wilting J, Weich HA. Mouse lung contains endothelial progenitors with high capacity to form blood and lymphatic vessels. *BMC Cell Biol*. 2010;11:50.
24. Baker CD, Ryan SL, Ingram DA, Seedorf GJ, Abman SH, Balasubramaniam V. Endothelial colony-forming cells from preterm infants are increased and more susceptible to hyperoxia. *Am J Respir Crit Care Med*. 2009;180:454–461.
25. Baker CD, Balasubramaniam V, Mourani PM, Sontag MK, Black CP, Ryan SL, Abman SH. Cord blood angiogenic progenitor cells are decreased in bronchopulmonary dysplasia. *Eur Respir J*. 2012;40:1516–1522.
26. Borghesi A, Massa M, Campanelli R, Bollani L, Tziella C, Figar TA, Ferrari G, Bonetti E, Chiesa G, de Silvestri A, Spinillo A, Rosti V, Stronati M. Circulating endothelial progenitor cells in preterm infants with bronchopulmonary dysplasia. *Am J Respir Crit Care Med*. 2009;180:540–546.
27. Schwartz SM, Benditt EP. Aortic endothelial cell replication. I. Effects of age and hypertension in the rat. *Circ Res*. 1977;41:248–255.
28. Schwartz SM, Benditt EP. Clustering of replicating cells in aortic endothelium. *Proc Natl Acad Sci U S A*. 1976;73:651–653.
29. Kunig A, Balasubramaniam V, Markham NE, Seedorf G, Gien J, Abman SH. Recombinant human VEGF treatment transiently increases lung edema but enhances lung structure after neonatal hyperoxia. *Am J Physiol Lung Cell Mol Physiol*. 2006;291:L1068–L1078.
30. Kunig AM, Balasubramaniam V, Markham NE, Morgan D, Montgomery G, Grover TR, Abman SH. Recombinant human VEGF treatment enhances alveolarization after hyperoxic lung injury in neonatal rats. *Am J Physiol Lung Cell Mol Physiol*. 2005;289:L529–L535.
31. Thébaud B, Michelakis E, Wu XC, Harry G, Hashimoto K, Archer SL. Sildenafil reverses O<sub>2</sub> constriction of the rabbit ductus arteriosus by inhibiting type 5 phosphodiesterase and activating BK(Ca) channels. *Pediatr Res*. 2002;52:19–24.
32. Fujinaga H, Baker CD, Ryan SL, Markham NE, Seedorf GJ, Balasubramaniam V, Abman SH. Hyperoxia disrupts vascular endothelial growth factor-nitric oxide signaling and decreases growth of endothelial colony-forming cells from preterm infants. *Am J Physiol Lung Cell Mol Physiol*. 2009;297:L1160–L1169.
33. Balasubramaniam V, Mervis CF, Maxey AM, Markham NE, Abman SH. Hyperoxia reduces bone marrow, circulating, and lung endothelial progenitor cells in the developing lung: implications for the pathogenesis of bronchopulmonary dysplasia. *Am J Physiol Lung Cell Mol Physiol*. 2007;292:L1073–L1084.
34. Balasubramaniam V, Ryan SL, Seedorf GJ, Roth EV, Heumann TR, Yoder MC, Ingram DA, Hogan CJ, Markham NE, Abman SH. Bone marrow-derived angiogenic cells restore lung alveolar and vascular structure after neonatal hyperoxia in infant mice. *Am J Physiol Lung Cell Mol Physiol*. 2010;298:L315–L323.
35. Yamada M, Kubo H, Kobayashi S, Ishizawa K, Numasaki M, Ueda S, Suzuki T, Sasaki H. Bone marrow-derived progenitor cells are important for lung repair after lipopolysaccharide-induced lung injury. *J Immunol*. 2004;172:1266–1272.
36. Ishizawa K, Kubo H, Yamada M, Kobayashi S, Numasaki M, Ueda S, Suzuki T, Sasaki H. Bone marrow-derived cells contribute to lung regeneration after elastase-induced pulmonary emphysema. *FEBS Lett*. 2004;556:249–252.
37. Ishizawa K, Kubo H, Yamada M, Kobayashi S, Suzuki T, Mizuno S, Nakamura T, Sasaki H. Hepatocyte growth factor induces angiogenesis in injured lungs through mobilizing endothelial progenitor cells. *Biochem Biophys Res Commun*. 2004;324:276–280.
38. Burnham EL, Taylor WR, Quyyumi AA, Rojas M, Brigham KL, Moss M. Increased circulating endothelial progenitor cells are associated with survival in acute lung injury. *Am J Respir Crit Care Med*. 2005;172:854–860.
39. Yamada M, Kubo H, Ishizawa K, Kobayashi S, Shinkawa M, Sasaki H. Increased circulating endothelial progenitor cells in patients with bacterial pneumonia: evidence that bone marrow derived cells contribute to lung repair. *Thorax*. 2005;60:410–413.
40. Fadini GP, Schiavon M, Cantini M, Baesso I, Facco M, Miorin M, Tassinato M, de Kreutzenberg SV, Avogaro A, Agostini C. Circulating progenitor cells are reduced in patients with severe lung disease. *Stem Cells*. 2006;24:1806–1813.

41. Schwarz TM, Leicht SF, Radic T, Rodriguez-Araboalaza I, Hermann PC, Berger F, Saif J, Böcker W, Ellwart JW, Aicher A, Heeschen C. Vascular incorporation of endothelial colony-forming cells is essential for functional recovery of murine ischemic tissue following cell therapy. *Arterioscler Thromb Vasc Biol.* 2012;32:e13–e21.
42. Lee C, Mitsialis SA, Aslam M, Vitali SH, Vergadi E, Konstantinou G, Sdrimas K, Fernandez-Gonzalez A, Kourembanas S. Exosomes mediate the cytoprotective action of mesenchymal stromal cells on hypoxia-induced pulmonary hypertension. *Circulation.* 2012;126:2601–2611.

### CLINICAL PERSPECTIVE

Preterm delivery is a major healthcare problem, affecting 10% of all births and accounting for > 85% of all perinatal complications and death. Each year, 5000 to 10000 newborns experience bronchopulmonary dysplasia, a chronic lung disease that follows ventilator and oxygen therapy for acute respiratory failure after premature birth. Bronchopulmonary dysplasia is characterized by the interrupted development of alveolar and vascular structures, and currently lacks specific therapeutic options. Alarming reports are now emerging suggesting that impaired lung development may manifest at adulthood leading to early-onset emphysema and pulmonary hypertension. Evidence suggests that angiogenesis contributes to alveolar growth. Here, we demonstrate that developing human and rat lungs harbor resident endothelial colony-forming cells, a subset of endothelial progenitor cells, capable of self-renewal and de novo vessel formation in vivo. Hyperoxia, a stimulus that contributes to bronchopulmonary dysplasia, perturbs human and rat lung endothelial colony-forming cell function in vitro and in vivo in experimental oxygen-induced bronchopulmonary dysplasia, respectively. Furthermore, exogenous, human cord blood–derived endothelial colony-forming cells restore normal lung alveolar and vascular growth and function and attenuate pulmonary hypertension. This effect is mediated through a paracrine effect. The improvement in lung structure and pulmonary hypertension persisted at 10 months with no adverse effects on lung structure and exercise capacity in hyperoxic-exposed animals. Human cord blood–derived endothelial colony-forming cells may represent a new therapeutic option for lung diseases characterized by impaired alveolar growth. These findings may ultimately extend to adult diseases associated with pulmonary hypertension or ischemic diseases.



**Existence, Functional Impairment, and Lung Repair Potential of Endothelial Colony-Forming Cells in Oxygen-Induced Arrested Alveolar Growth**

Rajesh S. Alphonse, Arul Vadivel, Moses Fung, William Chris Shelley, Paul John Critser, Lavinia Ionescu, Megan O'Reilly, Robin K. Ohls, Suzanne McConaghy, Farah Eaton, Shumei Zhong, Merv Yoder and Bernard Thébaud

*Circulation*. 2014;129:2144-2157; originally published online April 7, 2014;  
doi: 10.1161/CIRCULATIONAHA.114.009124

*Circulation* is published by the American Heart Association, 7272 Greenville Avenue, Dallas, TX 75231  
Copyright © 2014 American Heart Association, Inc. All rights reserved.  
Print ISSN: 0009-7322. Online ISSN: 1524-4539

The online version of this article, along with updated information and services, is located on the  
World Wide Web at:

<http://circ.ahajournals.org/content/129/21/2144>

Data Supplement (unedited) at:

<http://circ.ahajournals.org/content/suppl/2014/04/02/CIRCULATIONAHA.114.009124.DC1.html>

**Permissions:** Requests for permissions to reproduce figures, tables, or portions of articles originally published in *Circulation* can be obtained via RightsLink, a service of the Copyright Clearance Center, not the Editorial Office. Once the online version of the published article for which permission is being requested is located, click Request Permissions in the middle column of the Web page under Services. Further information about this process is available in the [Permissions and Rights Question and Answer](#) document.

**Reprints:** Information about reprints can be found online at:  
<http://www.lww.com/reprints>

**Subscriptions:** Information about subscribing to *Circulation* is online at:  
<http://circ.ahajournals.org/subscriptions/>

# SUPPLEMENTAL MATERIAL

## Existence, Functional Impairment And Lung Repair Potential of Endothelial Colony Forming Cells In Oxygen-Induced Arrested Alveolar Growth

**First Author: Alphonse**

**Short title: Endothelial colony forming cells for lung repair**

Rajesh S Alphonse, MD, PhD<sup>1</sup>, Arul Vadivel, PhD<sup>2</sup>, Moses Fung, BSc<sup>1</sup>, William Chris Shelley, BSc<sup>3</sup>, Paul John Critser, MD, PhD<sup>3</sup>, Lavinia Ionescu<sup>1</sup>, PhD, Megan O'Reilly<sup>1</sup>, PhD, Robin K Ohls<sup>4</sup>, MD, Suzanne McConaghy, MSc<sup>4</sup>, Farah Eaton, BSc<sup>1</sup>, Shumei Zhong, MSc<sup>2</sup>, Merv Yoder, MD<sup>3</sup>, Bernard Thébaud, MD, PhD<sup>2</sup>

<sup>1</sup> Department of Pediatrics, Women and Children's Health Research Institute, Cardiovascular Research Center and Pulmonary Research Group, University of Alberta, Edmonton, Canada

<sup>2</sup> Ottawa Hospital Research Institute, Regenerative Medicine Program, Sprott Center for Stem Cell Research, Department of Pediatrics, Children's Hospital of Eastern Ontario, University of Ottawa, Ottawa, Ontario, Canada

<sup>3</sup> Department of Pediatrics, Herman B Wells Center for Pediatrics Research, Division of Neonatal-Perinatal Medicine, Indiana University School of Medicine, Indianapolis, Indiana, USA

<sup>4</sup> Department of Pediatrics, University of New Mexico, Albuquerque, New Mexico, USA

**Correspondence:**

Dr. Bernard Thébaud  
Ottawa Hospital Research Institute  
501 Smyth Road  
Ottawa, ON K1H 8L6, Canada  
Phone: 613-737-8899, Fax: 613 739-6294  
E-mail: bthebaud@ohri

## **Materials and Methods**

All procedures were approved by the Animal Health Care Committee of the University of Alberta. Human fetal tissue collection was reviewed by the Institutional Review Board at the University of New Mexico and was determined to not constitute human subject research, as no identifying information was collected with tissues that would otherwise be discarded. The investigators collecting the tissues were not involved in the consent process and had no contact with women consenting to the termination procedure.

### **Lung ECFC isolation and culture**

Human fetal lungs (n=3, 17-20 weeks gestational age) were collected within 60 minutes after termination, washed in sterile PBS with antimicrobials, and suspended for further processing in a MEM with 10% FCS and antimicrobials. Rat lungs were collected at postnatal day (P)14 (n=5/group). Under aseptic conditions, the peripheral rims of the lungs were cut out, chopped into 1-2 mm<sup>2</sup> pieces and suspended in digestive solution (0.1 U collagenase and 0.8 U dispase/mL) (Roche Applied Science, Laval, QC) at 37 °C for 1 hr with intermittent shaking. The lung digest was strained through 70mm and 40mm cell strainers in tandem and washed twice with DMEM plus 10% fetal calf serum (FCS), at 300g and 4 °C for 10 min. After washing, the cells were resuspended in phosphate buffered saline (PBS) containing 0.1% (w/v) bovine serum albumin (BSA) and incubated with streptavidin tagged dynabeads (Dyna, Invitrogen, Burlington, ON) that were pretreated with biotinylated anti-rat or anti-human CD31 antibody (Abcam, Cambridge, MA). The dynabead tagged CD31 positive cells were selected using a magnetic separator and plated in a 6-well plate (4000-5000 cells/well) precoated with rat tail collagen type I and placed in a 37 °C, 5% CO<sub>2</sub> humidified incubator. After 24 hrs of culture, non-adherent cells and debris were aspirated, adherent cells were washed once and added with complete Endothelial Growth Medium-2 (cEGM-2). Medium was changed daily for 7 days and then every other day up to 14



days. ECFC colonies appeared as a well-circumscribed monolayer of cobblestone-appearing cells, between 5 and 14 days. ECFC colonies were identified daily from day 5 and enumerated on day 7 by visual inspection using an inverted microscope (Olympus, Lake Success, NY), under 20X magnification. Individual ECFC colonies were marked with a fine tipped marker and clonally isolated using cloning cylinders (Fisher Scientific, Ottawa, ON) and plated in T<sub>25</sub> flasks pretreated with collagen type I. Upon confluence, ECFCs were plated and expanded in type I collagen coated T<sub>75</sub> flasks. ECFCs between passages 4-8 were used for all experiments.

### **DiI-acetylated-low density lipoprotein (DiI-Ac-LDL) uptake and *Ulex europaeus*-lectin binding**

Attached cells at passage 4-5 were incubated with 20 µg/mL DiI-Ac-LDL (Biomedical technologies, Stoughton, MA) in cEGM-2 media for 4 hrs at 37 °C, 5% CO<sub>2</sub> in a humidified incubator. Cells were washed several times and fixed with 2% paraformaldehyde for 10 min. After washing with PBS, the cells were reacted with 10µg/ml fluorescein tagged *Ulex europaeus*-lectin (Vector Laboratories, Burlingame, USA) for 1h. Following nuclear counterstaining with Hoechst 33258, double-stained DiI-Ac-LDL<sup>+</sup>/FITC-Lectin<sup>+</sup> cells were imaged with an inverted fluorescence microscope (Leica Microsystems, Richmond Hill, ON, Canada).

### **Immunophenotyping of ECFCs**

Early passage (4-5) ECFCs (0.25-0.5 million per sample) were washed in flow buffer (PBS containing 0.05% sodium azide and 0.1% BSA) and blocked by incubation for 1 hr in 100µL of flow buffer containing 5% milk. ECFCs were then incubated at 4 °C for 30-60 minutes in dark with appropriate concentrations of primary or isotype control antibody, as outlined below, in 50µL of 5% milk-flow buffer. After washing, if necessary, the cells were incubated in dark, with comparable concentrations of secondary antibody in 50µL of 5% milk-flow buffer. After washing, antibody-labeled ECFCs were

analyzed by fluorescence-activated cell sorting (FACS) (FACSCalibur, BD Biosciences, San Diego, CA)<sup>1</sup>.

### **Retroviral mediated eGFP labelling of ECFCs**

By screening multiple Human Immunodeficiency Virus (HIV)-1 based lentiviral vectors for optimal transduction efficiency to ECFCs, we selected a vesicular stomatitis virus (VSV)-pseudotyped lentiviral vector harboring enhanced Green fluorescence protein (eGFP) under the control of ubiquitous Elongation factor (EF)-1 promoter (LV-EF-eGFP). Rat lung ECFCs in passage 4-5 were incubated overnight with  $2 \times 10^6$  TU/ml of lentiviral vector and 7  $\mu$ g/ml protamine sulfate in cEGM-2. ECFCs in wells with uniform green fluorescence were trypsinized, expanded and sorted for GFP fluorescence using FACS.

### ***In Vitro* Cell Viability Assay**

Lung ECFCs obtained from hyperoxia-exposed and room-air (control) rat pups were plated in equal numbers and grown in identical culture conditions. Cell viability was evaluated at various time points using the MTT assay as previously described.

### **Capillary-like network formation in Matrigel**

The formation of cord-like structures by ECFCs was assessed on Matrigel (BD Biosciences, Mississauga, ON) coated 96-well tissue culture plates as previously described<sup>2</sup>. The capillary-like networks were quantified by measuring the number of intersects and the total length of cord-like structures in random fields from each well using OpenLab (Quorum Technologies Inc, ON, Canada) software.

### **Single cell clonogenicity**

The FACSAria cell sorter (BD Biosciences, Mississauga, ON) was used to place one ECFC per well in a flat-bottomed 96-well tissue culture plate precoated with type I collagen and containing 200  $\mu$ L complete EGM-2 media. Cells were cultured at 5% CO<sub>2</sub> and 37 °C in a humidified incubator and culture media was replaced twice/week. At day 14, Hoechst 33258 (Sigma) was added at 3  $\mu$ g/mL to each well for 10 min for nuclear detection. The culture plate was examined with a fluorescent microscope at 20X magnification, well by well, for the growth of endothelial cells. Wells with 2 or more endothelial cells were scored as positive. The number of cells per well was enumerated by visual inspection at 40X magnification. Colonies with more than 500 cells were trypsinized and resuspended in cEGM-2. Based on the number of cells in that colony, an appropriate amount of cEGM-2 was added and mixed well such that each 200  $\mu$ L would approximately contain one ECFC. From this suspension, cells were again seeded at single cell density in 96-well plates precoated with collagen type-I, cultured for 2 weeks and evaluated for secondary colonies (or second generation colonies), as described earlier. ECFCs from colonies with more than 500 cells were serially passaged in 24-well and 6-well tissue culture plates followed by T<sub>25</sub> and T<sub>75</sub> tissue culture flasks.

### ***De novo angiogenesis in vivo***

ECFCs were loaded on collagen-fibronectin matrices and implanted subcutaneously in NOD/SCID mice to assess their capacity to contribute to *de novo* vasculogenesis as described<sup>3</sup>. ECFCs were identified by antibody specific for human CD31 (Dako, Carpinteria, CA) that cross-reacts with rat but no mouse endothelial cells. Cellularized collagen-fibronectin implants were excised after 14 days post-implantation and examined for vascularization by immunohistochemical staining. Red blood cell perfused anti-human CD31<sup>+</sup> vessels were identified in implants loaded with human or rat ECFCs respectively.

### **Oxygen-Induced BPD Model**

We used two rodent models of oxygen-induced BPD: 1) For comparison of lung ECFC function, newborn rat pups were exposed to room air (21%; control group) or hyperoxia (95% oxygen; BPD group) from birth to P14 in sealed Plexiglas chambers (OxyCycler; BioSpherix, Lacona, NY) with continuous oxygen monitoring and ECFCs were isolated at P14 for comparative analysis<sup>2</sup>; 2) To test the therapeutic potential of human cord blood-derived ECFCs, immune-compromised newborn rag<sup>-/-</sup> mice were exposed to 85% oxygen from P4 to P14. Human cord-derived ECFCs, isolated, expanded, and quality controlled as previously described<sup>1</sup> were administered at P14 through the jugular vein ( $10^5$  cells/mouse in 100  $\mu$ L DMEM). Lungs were harvested at P28. For cell engraftment experiments, ECFCs were labeled prior to injection with a red fluorophore (CellBrite<sup>TM</sup> Cytoplasmic Membrane Staining Kit, Biotium Inc, Hayward, CA). A subset of mice was kept for long-term assessment until 10 months of age.

### **Lung Morphometry**

Lungs were fixed with a 4% glutaraldehyde solution through the trachea under a constant pressure of 20 cm H<sub>2</sub>O. The trachea was ligated, and the lungs were immersed in fixative overnight at 4°C. Lung volume was measured by water displacement<sup>4</sup>. Lungs were embedded in paraffin and serial step sections, 4 mm in thickness, were taken along the longitudinal axis of the lobe. The fixed distance between sections was calculated so as to allow a systematic sampling of 10 sections across the whole lobe. Lungs were stained with hematoxylin and eosin (H&E). Alveolar structures were quantified on a motorized microscope stage (Leica CTRMIC and openlab software, Quorum Technologies; Guelph, ON) by using the mean linear intercept (MLI) as previously described<sup>2</sup>.

**Immunohistochemistry.** Sections were incubated with a polyclonal rabbit anti-von Willebrand Factor (vWF) antibody (Catalog #A0082; Dako) and a biotinylated secondary antibody (Catalog #B2770; Life Technologies Inc., Burlington, ON). A streptavidin-HRP conjugate (Catalog #S-911; Life Technologies



Inc., Burlington, ON) was used to link the DAB Chromogen (DAB Catalog # D4293; Sigma Aldrich, Oakville, ON) for visualization. Lung capillaries (30-100 $\mu$ m) were quantified on a motorized microscope stage.

### **Right Ventricular Hypertrophy**

The right ventricle free wall was separated from the left ventricle and the septal wall. The tissue was dried overnight and weighed the following day<sup>5</sup>.

### **Echocardiography**

All evaluations of pulmonary artery flow were performed with a (maximal) sweep speed of 200 mm/s. Pulsed-wave Doppler of pulmonary outflow was recorded in the parasternal view at the pulmonary valve level. The pulmonary acceleration time (PAAT) was measured from the beginning of the pulmonary flow to its onset and normalized with heart rate for comparisons as described<sup>5</sup>.

### **Lung function testing**

Tests were performed on anesthetized and paralyzed animals using Flexivent (Scireq, Montreal, QC, Canada) as described<sup>6</sup>.

### **Real-time PCR**

Total RNA was extracted from pulverized frozen lungs using Qiagen RNeasy kit (Qiagen, Mississauga, ON). RNA was quantified using a Nanodrop system (ND-1000 ThermoFisher Scientific, Wilmington, DE) and cDNA was prepared from lung RNA using random hexamers. PCR was performed on an ABI 7900 and using Taqman Universal PCR master mix (Applied Biosystems), Human Alu sequence primers and values were determined from a standard curve prepared from pure ECFCs to detect human cells. All results are expressed as a ratio of Alu sequences normalized to

human 18S. Three animals/group were harvested at 2 hours, 3, 7, 14 and 21 days after injection.

### **ECFC-derived Conditioned Media (CdM) experiments**

Human umbilical cord-blood ECFCs in passages 4-6 were grown in T<sub>75</sub> flasks up to 90% confluence in cEGM-2. Following removal of the respective culture medium, cells were rinsed 3 times with PBS and serum free DMEM was added. After 24 hours, supernatants were collected, concentrated (25x) and desalted by centrifugal filtration (Amicon - Millipore, Billerica, MA) as described<sup>6</sup>. Upon preparation, CdM was pooled, frozen at -80°C and thawed right before use. Control cell CdM was obtained from HUVECs.

*In vitro*, AT2 were isolated from time-dated fetal day 19.5 rat lungs as described using serial differential adhesions to plastic and low-speed centrifugations<sup>7</sup>. For wound healing assays, 10<sup>6</sup> cells/mL AEC2 were seeded into a plastic 24-well cell culture plate. At ~80 hours, the cell monolayer was scraped with a p200 pipette tip and media replaced with CdM or DMEM. The surface area of the wound was recorded over time using OpenLab (Quorum Technologies Inc, ON, Canada)<sup>7</sup>.

*In vivo*, CdM was administered daily to newborn rats exposed to hyperoxia through intraperitoneal injections at the dose of 7 µl/g<sup>6</sup> from P4 to P21 and lungs were harvested at P22.

### **Exercise capacity**

Mice were run according to a predetermined protocol. Exhaustion was defined as the animal running exclusively on the lower third of the treadmill coupled with hitting of the shock panel twice within 30 seconds<sup>6</sup>.

### **Statistical Analysis**

Values are expressed as means ± standard error of the mean (SEM). Statistical comparisons were made with ANOVA. *Post hoc* analysis used Fisher's probable least significant difference test (Statview 5.1;

Abacus Concepts, Berkeley, CA). A value of P less than 0.05 was considered statistically significant.

All endpoints were assessed by investigators blinded to the experimental groups.

Figure S-1

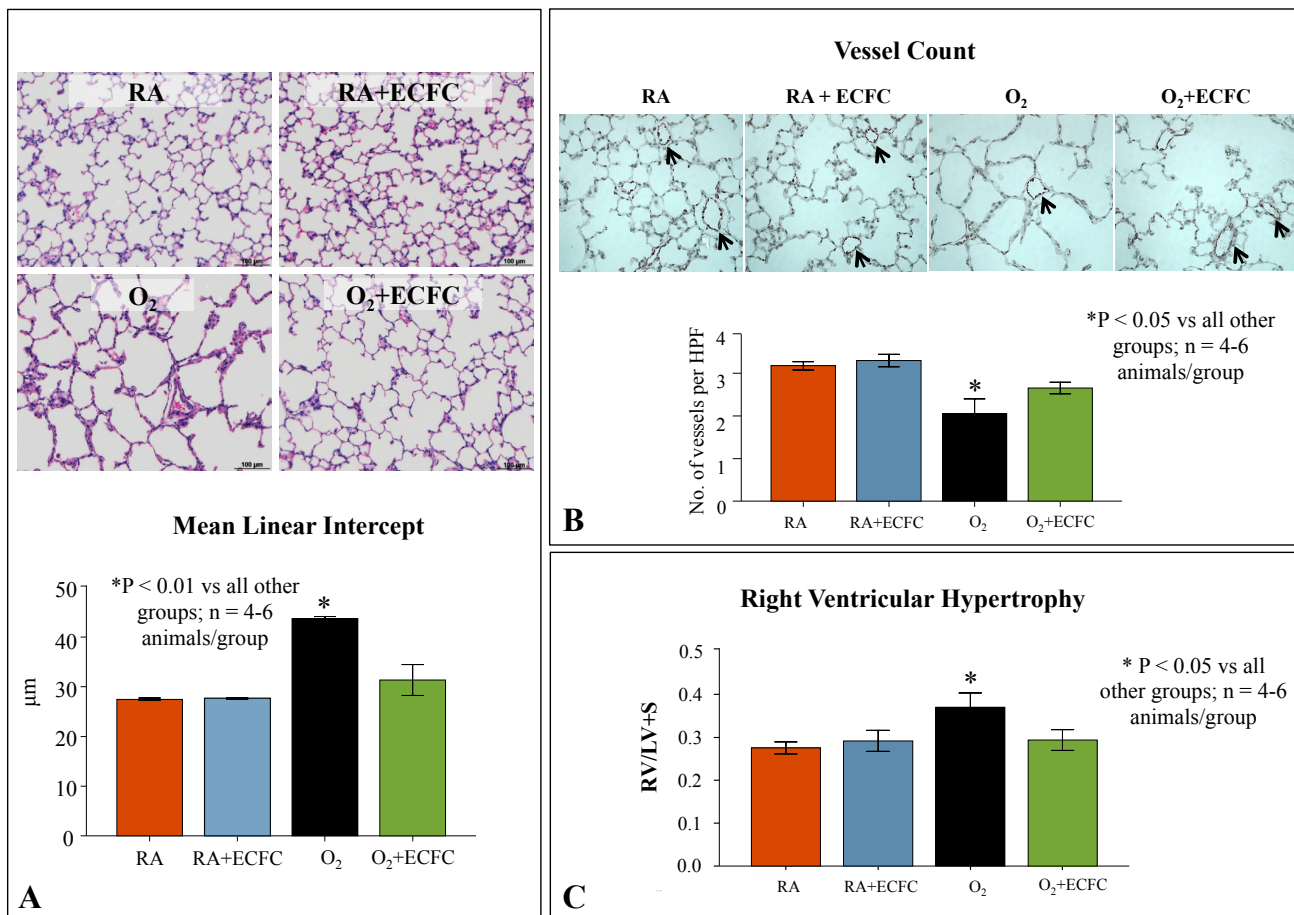
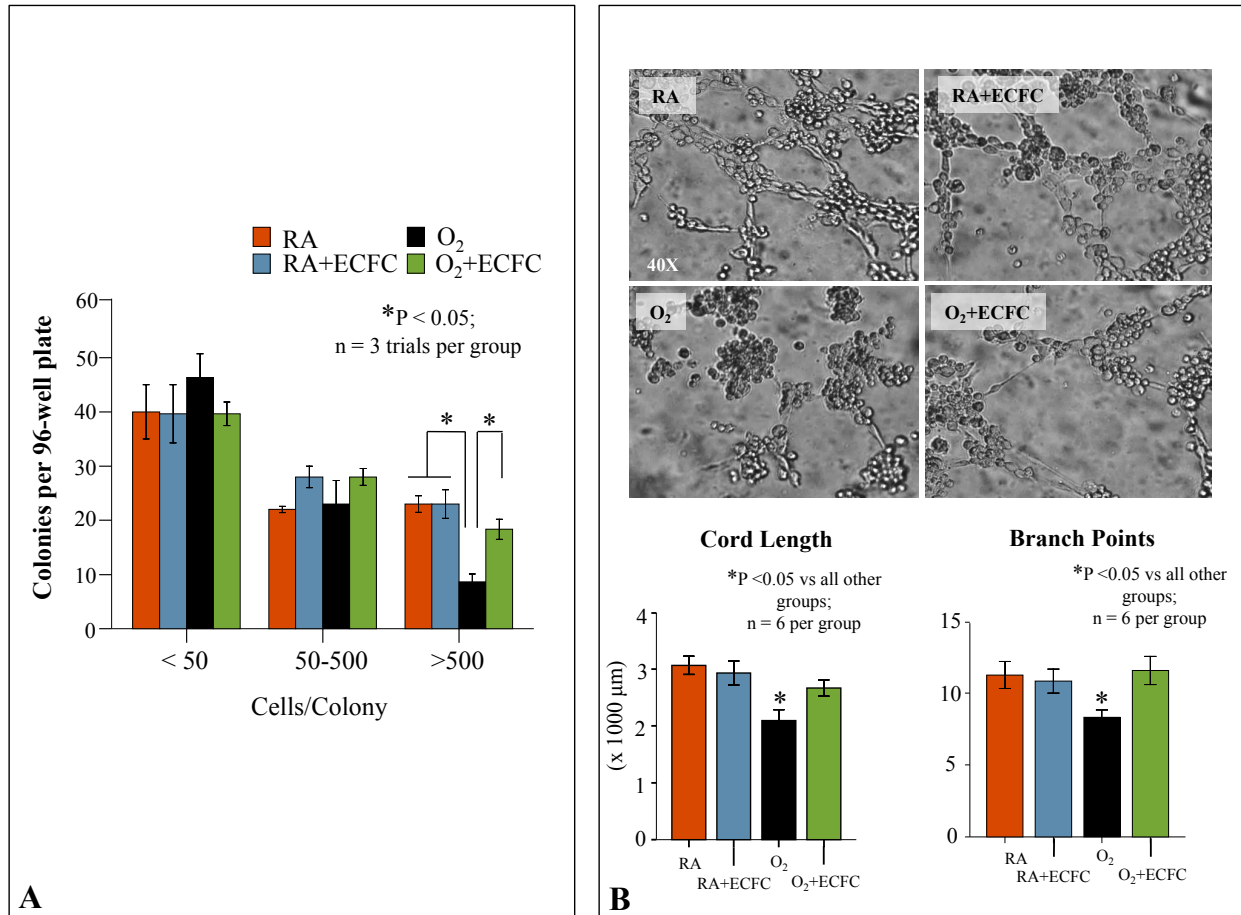




Figure S-2



## Supplemental Figure Legends

**Figure S-1. Human umbilical cord ECFC therapy reverses alveolar and lung vascular growth arrest and attenuates RVH in hyperoxia-exposed newborn RNU rats.** **A.** Representative H&E-stained lung sections at P28 show the characteristic arrested alveolar growth with larger and fewer alveolar structures in untreated hyperoxia-exposed ( $O_2$ ) lungs as compared to control rats housed in RA. Intra-jugular administration of ECFCs in  $O_2$ -exposed animals restored alveolar growth as compared to untreated  $O_2$ -exposed animals. Quantitative assessment of alveolar architecture by the mean linear intercept confirms the protective effect of ECFCs on alveolar growth compared to untreated  $O_2$ -exposed animals (n=4-6/group, \*P<0.01). ECFCs did not alter lung structure in control RA rats. **B.** Effects of ECFC treatment on pulmonary vessel density assessed on lung sections stained with von Willebrand Factor (vWF) at P28. Pulmonary vessel density of 30-100 $\mu$ m sized blood vessels per 10 high power fields (40X) was significantly decreased in the lungs of  $O_2$ -exposed rats compared to RA. Intra-jugular injection of ECFCs significantly improved pulmonary vessel density compared to untreated  $O_2$ -exposed animals (n=4-6/group, \*P<0.05). **C.** Hyperoxia-exposed rats displayed significant RVH compared to RA housed animals as indicated by the increase in right ventricle/left ventricle plus septum (RV/LV+S) ratio compared with controls. ECFC therapy significantly reduced RVH in hyperoxic exposed rats compared to untreated  $O_2$ -exposed rats (n=4-6/group, \*P<0.05).

**Figure S-2. Human umbilical cord ECFC therapy restores resident lung ECFC function in hyperoxia-exposed newborn RNU rats.** **A. Comparative single cell clonogenic assay.** Colony forming potential of single plated ECFCs from RNU rat lungs was assessed by measuring the percentage of single ECFCs capable of generating colonies after 14 days in culture. Significantly fewer ECFCs from the hyperoxia group were capable of generating colonies with 500 or more cells in comparison with RA controls (\*P<0.05, n=3 trials/group). Treatment with cord blood-derived ECFCs

significantly restored the colony forming potential of resident lung ECFCs isolated from treated RNU lungs exposed to hyperoxia (\*P<0.05, n=3 trials/group). Cell therapy did not alter the colony forming properties of ECFCs from control RA rat lungs. **B. Quantitative assessment of the *in vitro* capillary-like network forming ability of lung ECFCs.** Lung resident ECFCs from untreated hyperoxic rats formed fewer capillary networks compared to lung ECFCs from untreated hyperoxia-exposed rats as assessed by the cord length and number of branch points (n=6/group, \*P<0.05). Cord blood ECFC therapy restored the ability of hyperoxic resident lung ECFCs to form capillary-like networks as assessed by improved total cord length and number of intersects compared to lung ECFCs from untreated hyperoxia-exposed RNU rats (n=6/group, \*P<0.05).

## References

1. Mead LE, Prater D, Yoder MC, Ingram DA. Isolation and characterization of endothelial progenitor cells from human blood. *Curr Protoc Stem Cell Biol.* 2008;Chapter 2:Unit 2C 1
2. Thebaud B, Ladha F, Michelakis ED, Sawicka M, Thurston G, Eaton F, Hashimoto K, Harry G, Haromy A, Korbitt G, Archer SL. Vascular endothelial growth factor gene therapy increases survival, promotes lung angiogenesis, and prevents alveolar damage in hyperoxia-induced lung injury: Evidence that angiogenesis participates in alveolarization. *Circulation.* 2005;112:2477-2486
3. Yoder MC, Mead LE, Prater D, Krier TR, Mroueh KN, Li F, Krasich R, Temm CJ, Prchal JT, Ingram DA. Redefining endothelial progenitor cells via clonal analysis and hematopoietic stem/progenitor cell principals. *Blood.* 2007;109:1801-1809
4. Scherle W. A simple method for volumetry of organs in quantitative stereology. *Mikroskopie.* 1970;26:57-60
5. Ladha F, Bonnet S, Eaton F, Hashimoto K, Korbitt G, Thebaud B. Sildenafil improves alveolar growth and pulmonary hypertension in hyperoxia-induced lung injury. *Am J Respir Crit Care Med.* 2005;172:750-756
6. Pierro M, Ionescu L, Montemurro T, Vadivel A, Weissmann G, Oudit G, Emery D, Bodiga S, Eaton F, Peault B, Mosca F, Lazzari L, Thebaud B. Short-term, long-term and paracrine effect of human umbilical cord-derived stem cells in lung injury prevention and repair in experimental bronchopulmonary dysplasia. *Thorax.* 2013;68:475-484
7. van Haaften T, Byrne R, Bonnet S, Rochefort GY, Akabutu J, Bouchentouf M, Rey-Parra GJ, Galipeau J, Haromy A, Eaton F, Chen M, Hashimoto K, Abley D, Korbitt G, Archer SL, Thebaud B. Airway delivery of mesenchymal stem cells prevents arrested alveolar growth in neonatal lung injury in rats. *Am J Respir Crit Care Med.* 2009;180:1131-1142



